An Investigation of the Diels-Alder Reaction of 2,4–Hexadiene with Sulfur Dioxide and a Novel Procedure for Non-Orthogonal Localisation of Molecular Orbitals

Richard Lynn Dustin Bryant

M.Sc.

The University of York
Department of Chemistry

January 2012

Abstract

This thesis is divided into four parts, which reflect the various components of the research covered. The introductory section covers the essential, basic quantum chemistry necessary for any fruitful study in the subject; a review of necessary tools is given which ranges in topic from the presentation of Schrödinger's equation for many-body theory to density functional theory versus perturbation theory. After a clear exposition of these topics, their practical implementation to characterise the Diels-Alder reaction of 2,4-hexadiene with sulfur dioxide is described. This theoretical study is rooted in the experiments on the same reaction; additionally, a previous – albeit, more elementary – theoretical study was also completed by another group. The work herein is distinct in two ways: first, all possible isomers of the diene were investigated; secondly, the reactions were studied with greater accuracy and results were compared using different methods. Additionally, the molecular orbitals of the reaction were localised using standard techniques in the literature. The third section of the thesis is devoted to clearly covering a series of numerical methods which can be used to solve common problems encountered in quantum chemistry. A discussion of the strengths and weaknesses of each method is also given. Although, it is true that many of these methods are implemented in stable quantum chemistry packages, these methods were primarily discussed in light of their potential application for solving the, yet unresolved, issue of constructing highly localised non-orthogonal molecular orbitals. To date, localised molecular orbitals are constructed as linear combinations of atomic orbitals with the restriction that the molecular orbitals form an orthonormal set; while mathematically convenient, the constraint that the set be orthogonal is unrealistic and its removal should allow for constructing non-orthogonal LMOs. Presented is an original solution to Boys' functional for optimising the construction of non-orthogonal molecular orbitals.

Every attempt to employ mathematical methods in the study of chemical questions must be considered profoundly irrational and contrary to the spirit of chemistry.... if mathematical analysis should ever hold a prominent place in chemistry – an aberration which is happily almost impossible – it would occasion a rapid and widespread degeneration of that science. – **Auguste Comte**

Contents

List of Figures

List of Tables

Acknowledgements

I dedicate this thesis to my Mom and grandfather, they have been very supportive of my studies and I know I would not have been able to do any of this without them.

Author's declaration

This research was carried out at the University of York between October 2010 and December 2011 and to the best of my knowledge is original save when reference is made to outside sources.

Chapter 1

Introduction

From antiquity, there has been an interest in understanding the fundamental laws that govern the universe; science, necessarily, developed to rigorously attempt to answer these questions. Towards the end of the nineteenth century many zealous physicists believed that nearly all the fundamental questions of the universe had been answered and it was only a matter of time before we had a theory to explain everything. However, a series of experiments began to show that our universe and its governing laws are more complicated than they appear at first glance. Many of their results began to blur the lines between chemistry and physics; in particular, Rutherford's experiment and the discovery of wave-particle duality truly changed our understanding of what matter is. Chemistry, on the other hand, with its own rich history tended to avoid the pursuit of mathematical formulae, which often leads physicists to reductionism. Classical chemistry concerned itself with mixing and creating new substances, which is at the heart of modern industrial chemistry with a significantly improved grounding. Perhaps the biggest problem, and what ultimately brought these seemingly separate fields together, was rigorously predicting chemical reactions through the chemical bond; equivalently, chemists began to realise that structure and reactivity were highly correlated. However, chemists had not yet understood true structure or why molecules united, or what that really meant until the concept of a chemical bond was born. It is the goal of this present work to attempt to clearly elaborate the concept of a chemical bond, and show that this can be done in a very precise mathematical framework. In doing this we will rigorously connect the idea of bonding with molecular orbitals and also illustrate how electronic structure can explain many chemical phenomenon.

In classic physics, we have a few axioms, Newton's laws, which explain the relationship between mass and energy

$$E = T + V$$

$$E = \frac{mv^2}{2} + V \tag{1.1}$$

$$E = \frac{p^2}{2m} + V$$

To view chemistry through the eyes of physics, we must apply a similar equation. Radically, though, matter does not behave in a way which is predicted according to Newton's laws at the micro scale, which is the setting we must take when approaching the chemical bond. In 1926, Erwin Schrödinger showed that if one fixes the dimension of time, a one-dimensional quantum particle behaves according to:

$$E\psi = -\frac{\hbar^2}{2m}\frac{\partial^2\psi}{\partial x^2} + V(x) \tag{1.2}$$

where ψ is the solution to the equation and is a function of position, x [34, Chapter 2]. There is actually considerable similarity between these equations: $\frac{\hbar^2}{2m}\frac{\partial^2\psi}{\partial x^2}$ coincides with $\frac{p^2}{2m}$ and they both have mass dependency. The next step in any physics problem is to consider the system and its setting for formulating solutions. Heuristically, one can view the wave function, for a simple atom, H, system as the solution path or place that its electron occupies; whether or not the wave function has any true physical interpretation is outside the scope of this thesis and I leave such answers to philosophers. Moving to a two-electron system, helium, we introduce an additional variable:

$$\left\{ -\frac{1}{2}(\nabla_1^2 + \nabla_2^2) - Z\left(\frac{1}{r_1} + \frac{1}{r_2}\right) + \frac{1}{r_{1,2}} \right\} \phi(r_1, r_2) = E\phi(r_1, r_2) \tag{1.3}$$

where Z is the atomic number of the atom involved. Fortunately, this equation cannot be solved in closed form and it is the last piece in brackets that gives birth to quantum chemistry – a blend of physics, chemistry, and most importantly, applied mathematics. The part in brackets is known as the electronic Hamiltonian, it is the operator we consider when searching for suitable wave-functions; when applied tw molecules it is only an approximate Hamiltonian in that it ignores contributions of chemical bond vibration and rotation (known as the Born-Oppenheimer approximation), as well as relativity and quantum electrodynamics [34, Chapter 2]. We shall refer to the electronic Hamiltonian simply as the Hamiltonian in this thesis. In some way, quantum chemistry is nothing more than solutions to a generalised Schrödinger equation, yet there are deep assumptions that we make in developing these solutions that must be grounded solidly and there are subtle tricks we employ to implement these ideas in a practical manner.

1.1 Formalism of Quantum Chemistry

As stated previously, one approach to studying the electronic structure of systems is to simplify their Hamiltonians and then calculate the energy of such a system. If the Hamiltonian is treated as a sum of simple Hamiltonians, a simple approximation comes out:

$$H = h_1(r_1) + h_2(r_2) + \frac{1}{r_{1,2}} \cong h_1(r_1) + h_2(r_2) \tag{1.4}$$

This is the independent particle model and actually a toy example of the variational method, which was used extensively in our research [34, Chapter 7]. The proof of the variational method is really quite straightforward and worth investigating for its insight [39, Chapter 1.3]:

$$\int f^* f \, d\tau = 1 \rightarrow \int f^* H f \, d\tau \geq E_0 \tag{1.5}$$

We can assume that there exist solutions for the Schrodinger equation:

$$H\psi_i = E_i \psi_i \tag{1.6}$$

Furthermore, the space is complete so any function can be expressed as a linear combination of its basis functions:

$$f = \sum_i c_i \psi_i \tag{1.7}$$

$$\int f^* H f \, d\tau = \sum_i |c_i|^2 \int \psi_i^* H \psi_i \, d\tau = \sum_i |c_i|^2 E_i \geq E_0 \sum_i |c_i|^2 \tag{1.8}$$

$$\int f^* f \, d\tau = \int \left(\sum_i c_i \psi_i\right)^* \left(\sum_j c_j \psi_j\right) d\tau = \sum_i |c_i|^2 \delta_{i,j} = 1 \tag{1.9}$$

$\delta_{i,j}$ is merely a result of choosing the basis set in such a way that the components are orthonormal, but this immediately forces $\sum_i |c_i|^2 = 1$ so that what we have proven the result. The result of this proof is independent of the choice of the trial wave-function used; this means, practically, that any wave-function will do, and our intuition and experience should aide us in our constructions of such functions. Quantum chemical methods that employ the variational method essentially seek to find a wave-function that gets the energy as low as possible; after all, the energy is bounded below by the exact wave-function's energy. The other major tool in quantum chemistry is perturbation theory. Using perturbation theory, one attempts to find a Hamiltonian which is close to the Hamiltonian of interest. Rather than optimizing trial wave-functions through a known Hamiltonian, we choose Hamiltonians

so we can find *exact* eigenfunctions and their eigenvalues (energy). The premise of perturbation theory is that any Hamiltonian, H can be written in parts:

$$H = H^0 + \lambda P \tag{1.10}$$

where λP is the perturbation term and H^0 is some expression we can represent analytically and quickly solve. If the perturbation is small then the equations will look like [27, Chapter 9]:

$$H^0 \psi_i + \lambda P \psi_i = E_i \psi_i : \lambda \to 0 \tag{1.11}$$

$$\left(H^0 + \lambda P - E_i \right) \psi_i = 0 \tag{1.12}$$

In general however, one may consider an analytical wave-function to consist of an infinite series of parts, or 'perturbations':

$$\psi_i = \psi_i^0 + \sum_{j=1}^{\infty} \lambda^j \psi_i^{(j)} \tag{1.13}$$

$$E_i = E_i^0 + \sum_{j=1}^{\infty} \lambda^j E_i^{(j)} \tag{1.14}$$

Where $H\psi_i \equiv (H^0 + \lambda P) \left(\lambda^0 \psi_i^{(0)} + \lambda \psi_i^{(1)} + \lambda^2 \psi_i^{(2)} + \cdots \right) = \left(E^{(0)} + \lambda E^{(1)} + \cdots \right) \psi_i$, we see that a simple, albeit infinite, set of equations is formed when we multiply through and collect term of similar powers of lambda:

$$\left(H^0 - E_i^0 \right) \psi_i^0 = 0$$

$$\left(H^0 - E_i^0 \right) \psi_i^{(1)} + \left(P - E_i^{(1)} \right) \psi_i^0 = 0 \tag{1.15}$$

$$\left(H^0 - E_i^0 \right) \psi_i^{(2)} + \left(P - E_i^{(1)} \right) \psi_i^{(1)} - E_i^{(2)} \psi_i^0 = 0$$

$$\vdots$$

Solved in succession, one can get a closer solution each time; each term in the infinite series is another order of perturbation. For example, the first iteration is the 0-th perturbation, the third term is 2nd order perturbation. An example of a perturbation approximation would be, equation, (1.4).

Chapter 2

The Hartree-Fock Method and other techniques

As stated previously, the molecular wave-function is constructed as linear combinations of the basis functions; naturally, one asks what the basis functions are. One popular method is to express the simplest molecular wave-function as a Slater determinant[24, p. 58]:

$$\psi(x_1, \ldots, x_n) = \frac{1}{\sqrt{n!}} \begin{vmatrix} \chi_1(x_1) & \cdots & \chi_n(x_1) \\ \vdots & & \vdots \\ \chi_1(x_n) & \cdots & \chi_n(x_n) \end{vmatrix} \tag{2.1}$$

$$\psi(x_1, x_2) = \chi_1(x_1)\chi_2(x_2) \tag{2.2}$$

$$\psi(x_1, x_2) = \frac{1}{\sqrt{2}} \left(\chi_1(x_1)\chi_2(x_2) - \chi_1(x_2)\chi_2(x_1) \right) \tag{2.3}$$

Equation (2.2) is the Hartree product for a two particle system, while (2.1) is a generalisation of (2.3) which also factors in a normalization condition, $\frac{1}{\sqrt{n!}}$, and has the property that an exchange of any pairs of rows or columns changes the sign of the equation and satisfies the Pauli principle. Notice that (2.3) is really just (2.2) but considering a system in which the particles are indistinguishable (i.e. $\psi(x_1, x_2) = -\psi(x_2, x_1)$), and therefore takes an antisymmetric combination of both possibilities.

Given that one can express a molecular orbital as a linear combination of basis functions and also that such a trial function will satisfy the certain bounds (1.5), there is still the pressing issue of optimizing the functions, . If the basis functions are chosen to be atomic-like orbitals then our intuition of molecular chemistry will fit

appropriately. The atomic orbitals are themselves functions of spatial orientation, so a method that can accurately describe a set of molecular orbital must both treat the molecular orbitals as functions of all atomic orbitals and each atomic orbital as a function of position [39, p. 181]. In the Hartree-Fock method, the optimal orbitals are calculated through a self-consistent field procedure. The Hamiltonian for m-electrons is [34, p. 127]:

$$H = -\frac{1}{2}\sum_{i=1}^{m}\nabla_i^2 - \sum_{i=1}^{m}\frac{Z}{r_i} + \sum_{i=1}^{m}\sum_{j<i}^{m}\frac{1}{r_{i,j}} \tag{2.4}$$

which is applied in the generalised Schrodinger equation:

$$H\psi(r_1, \ldots, r_m) = E\psi(r_1, \ldots, r_m) \tag{2.5}$$

The so-called Hartree-Fock (HF) method becomes self-consistent through optimising the energy of a Slater determinant. Looking at only the ith electron in an m-electron system, the Fock operator is [34, p. 133]:

$$F(i) = -\frac{\nabla_i^2}{2} - \frac{Z}{r_i} + \sum_{j=1}^{m}[2J_j(i) - K_j(i)] \tag{2.6}$$

Clearly, the operator applied to the full system of electrons takes on a general form:

$$F(i)\chi(i) = \epsilon(i)\chi(i) \tag{2.7}$$

J is the Columb operator, $J_b(1) = \int |\chi_b(2)|^2 r_{12}^{-1}\,d\tau_2$ and K is the exchange operator, $K_b(1)\chi_a(1) = \left[\int \chi_b^*(2)r_{12}^{-1}\chi_a(2)\,d\tau\right]\chi_b$ [39, p. 114]. The key observation we need to take away from the definitions of these operators, J and K, is that they make each one-electron function dependent on the entire system and therefore the system of equations are highly non-linear because the Fock operator in turn is composed of the orbitals. The method presented here is known as the closed-shell HF method and is designed for molecular (and atomic) orbitals which have no unpaired electrons. There are two other methods used in the case of open shells, the Restricted open-sheel Hartree-Fock (ROHF) and the Unrestricted Hartree-Fock (UHF) methods. In any of the cases, the method operates iteratively until the set of orbitals, $\{\chi_i\}$, does not change – becomes self consistent. As a result of becoming convergent, the Slater determinant (energy) is minimised.

Without ever explicitly saying what the atomic orbitals were (other than they have a spatial component), we have defined them as the basis for constructing molecular orbitals, and see that they can be optimized through transformations via the HF

method. In fact, any choice of 'atomic orbitals' is allowed but commonly we use the Gaussian orbitals [24, p. 15]:

$$g = r^{n-1}e^{-(\alpha r^2)}Y_{lm}(\theta, \phi) : \text{fixed } \alpha \in \mathbb{R} \qquad (2.8)$$

where n is the principal quantum number, r is the position operator, and $Y_{lm}(\theta, \phi)$ stands for the spherical harmonic function. Other orbitals that have been used include the Slater orbitals which look like hydrogen orbitals; however they are usually only useful for linear molecules. The atomic orbitals can be chosen as linear combinations of the Gaussian orbitals which, in turn, approximate Slater orbitals [34, p. 165]:

$$\chi_\mu = \sum_\rho^K c_{\mu,\rho} g_\rho \qquad (2.9)$$

The convention being that the number is used in naming the basis set STO-KG. However, more commonly we use the k-k'k''G Split-Valence basis sets, where k designates the number of Gaussian-like orbitals used to construct the inner shell for the given atom centre, while the k'k'' numbers describe the valence electrons of an atom. For example, the valence electrons can be represented as a linear combination of Slater-like functions, with different choice of zeta, ζ [24, p.158]:

$$\text{valence} = Ae^{-(\zeta_1 r)}r^{n-1}Y_{lm}(\theta, \phi) + Be^{-\zeta_2 r}r^{n-1}Y_{lm}(\theta, \phi) \qquad (2.10)$$

A common basis choice is 6-31G, which uses six Gaussians to represent the inner-shell, three Gaussians in one set of the valence and one Gaussian for the other set. Given any basis function, one can add additional diffuse (d) or polarization (p) functions; using the basis set we just discussed, this addition would be represented as 6-31G(d,p). Our research employed the set 6-311G(d,p) most commonly (valence of three sets of size three, one and one). In practice it is convenient to first perform a crude calculation using small basis sets with simple methods like Hartree-Fock, then transferring the optimised results to a higher level of theory for more accurate treatment.

The Hartree-Fock method is only a first approximation although the rationale behind its use is critical for having a good understanding of what quantum chemical calculations should do. Previously we studied the idea of perturbation theory in a very abstract and general setting; however, perturbation theory has a very fruitful setting with Møller-Plesset (MP) perturbation theory. MP theory was developed in 1934 by Møller and Plesset [29] however it was not applied to chemical models until 1975 by Barlett [5] and Pople in 1976 [33]. The orders (refer to equations (1.15)) of the MP method are written MPn, and the 0th is defined as follows[29]:

$$E(MP0) = \sum_{i=1}^m \epsilon_i \qquad (2.11)$$

$E(MP0) + E(MP1)$ is merely the Hartree-Fock energy, the best result using only a Hartree-Fock calculation. However, we can begin to get perturbation corrections for order two and higher. The form of the second order correction is[29]:

$$E(MP2) = \sum_{i<j}^{occ} \sum_{a<b}^{vir} \frac{[\langle \phi_i \phi_j | \phi_a \phi_b \rangle - \langle \phi_i \phi_j | \phi_b \phi_a \rangle]}{\epsilon_i + \epsilon_j - \epsilon_a - \epsilon_b} \tag{2.12}$$

$$\langle \phi_i \phi_j | \phi_a \phi_b \rangle \equiv \int \phi_i(1) \phi_j(2) (r_{12})^{-1} \phi_a(1) \phi_b(2) dr_1 dr_2 \tag{2.13}$$

where the integral is known as the two electron integral and is useful in other applications, as well. While there are higher order approximations (MP3,MP4,), our research only conducted MP2 calculations and it is worth noting that the values of the energies converge in a zigzag pattern towards the actual solution ad infinitum [24, p. 131]. One key distinguishing feature of MPn calculations (and perturbation in general) is that no new wave-functions are constructed; rather, electron correlations are corrected for more terms through the perturbation expansion. This is why the calculated energy is not an upper bound to the exact Schrödinger equation's energy; however, as we shall soon see there is another method that is a widely-used variation of DFT (Density Functional Theory) that has some variational elements. The Becke, three-parameter, Lee-Yang-Parr (B3LYP) method is a hybrid model which is composed of multiple equations[38]:

$$E_{xc}^{B3LYP} = (1 - a_0) E_x^{HF} + a_x \Delta E_x^{B88} + a_c E_c^{LYP} + (1 - a_c) E_c^{VWN} \tag{2.14}$$

where $a_0 = .2$, $a_c = .81$, and $a_x = .72$. For a complete description of the functions implicit to E_{xc}^{B3LYP} reference the article in bibliography [38][24, Chapter 6].

2.1 Basis Set Superposition Errors

No discussion of bases would be complete without exposing their limits. The number one issue with any choice of basis is that it is finite and therefore incomplete. The obvious solution is to simply add more basis functions to a calculation, however this is not practical because computational effort is proportional to the fourth power (or worse) of the basis set size; therefore, the number of functions in a basis is typically several hundred, occasionally to a few thousand [24, pp. 172-173]. One obvious consequence of finite basis sets is the need to report the energies (of parts of reactions) using the same approximate basis; otherwise, comparisons are nonsensical. Further, when molecules are brought in close proximity to one another, the van der Waals interaction becomes more evident and basis functions between neighbours

become highly overlapped; this is to say that, near molecules begin to behave like one entity rather than two. The Counterpoise (CP) correction is a good approach towards analysis of basis set superposition error (BSSE).

In this next section we will discuss geometry optimisation in both a heuristic and exact manner, but for now let us simply assume that we can compute the geometry associated with a molecule. It should be obvious that the geometry of a part of a molecule isolated is different than the geometry of the whole because of intramolecular interactions. The CP method attempts to approximate BSSE by looking at the differences of energy between the parts and the whole, while considering associated geometries and bases [24, pp. 172-173]:

$$\Delta E_{complexation} = E(AB)_a^* b - E(A)_a - E(B)_b \tag{2.15}$$

Where the AB^* complex has basis set ab, molecule A has basis set a, and molecule B has basis set b Now to consider the basis overlap contributions, we treat each part as it were in the whole with all the bases but without the other parts' nuclei – known as ghost atoms – then subtract individual contributions to attempt to deduce redundancy:

$$\Delta E_{CP} = (E(A)_{ab}^* + E(B)_{ab}^*) - (E(A)_a^* + E(B)_b^*) \tag{2.16}$$

In the first parenthesis, we have each part's geometry treated as it appears in the whole with both of the bases contributing in each case, while in the second parenthesis, we have each part as its geometry appears in the whole but with only its own basis determining the energy. The reader should note that in the case of $E(A)_a^*$, for example, that the geometry is fixed and energy is calculated with a basis that would otherwise render $E(A)_a$ if the HF method was applied without a totally fixed geometry. Finally, $\Delta E_{corrected} = \Delta E_{complexation} - \Delta E_{CP}$ and we note that in the more general case of more parts, one would take many sums and differences. The error is always present and the CP technique merely approximates a correction, and notably does not give an analytical lower or upper bound to these errors. Like most quantum chemists, we ignore intramolecular (internuclear) BSSE, error due to basis functions on atoms within the same reactant; although, this error exists as well, there is not a consistent definition [24, pp. 172-173].

2.2 Geometry Optimisation

Having seen how the HF method operates, we wish to investigate how this is practical to the experimentalist who wishes to carry out ordinary chemistry. Chemists are often interested in the geometry of a molecule, because they can use this information to understand things such as steric hindrance, effects from certain functional groups,

and so on. Geometry is essential to modern chemistry because without it, chemical bonding delves into a mystery. Recall, that the wave-function, itself, is a function of the position of atoms and electrons, so there is a direct connection between the geometry of a chemical and its solution to Schrödinger's equation, implicit to the electronic structure. Solving the Fock equation is equivalent to finding a wavefunction which minimizes the ground state energy (E) of a molecule.

Before going into more complicated problems of arbitrary chemicals, we should consider simple one and two dimensional problems to geometry. A pair of classic examples – which are still being investigated in recent times – are the potential energy curve of the hydrogen molecule cluster [40] and the hydrogen molecule. In the former the molecules positions are treated as variables (with fixed intramolecular nuclear coordinates) much like the atoms are treated variable in the latter. In the latter, one can imagine the hydrogen atoms as points and the only geometry associated between them is a line (the chemical bond) which can be elongated or shortened; geometry optimisation is really this simple and this hard. If the atoms are brought too near to each other, the energy becomes high and the atoms are pushed away, the opposite is true for the atoms going too far from each other. It should be noted that while the optimised geometries of molecules are static, molecules such as water obviously do vibrate but there does exist a most relaxed geometry around which it oscillates like a spring. Water is a bit different, in that it is the simplest non-trivial molecule whose optimisation can be accelerated by choice of coordinates. The wave-function can be formulated equivalently as $\psi = \psi(\mathbf{x_0}, \mathbf{x_{H_1}}, \mathbf{x_{H_2}})$ or $\psi = \psi(r_{OH}, \theta_{H_2O})$, where $\mathbf{x_i} = [x_i, y_i, z_i]$ and r_{OH} is the distance from a hydrogen atom to oxygen and θ_{H_2O} is the angle of the bent water structure. When actually carrying out the calculation, one can impose symmetry so that the distance from one hydrogen to oxygen is the same distance from the other hydrogen to oxygen, by using the same variable, r_{OH}, when describing this function – this could not be done in ordinary Cartesian space. Effectively, we have reduced a problem of nine variables in three dimensional space to a problem of two variables.

Having spent a great deal discussing methods, basis sets, and a simple heuristic example with water, it is appropriate now to investigate potential energy surfaces in a precise sort of language. A first exposure to reaction-energy graphs is usually presented in very plain language: reactants, intermediates, all transition states, and products are 'points' on the independent axes and their associated energy on a dependent axis. However, in reality this is a very simple and crude picture of a chemical reaction. A chemical reaction in the mathematical sense is merely a minimum energy curve following the potential energy surface with the atomic coordinates as the many dimensions of the function. Except for the most simple of chemical systems, a full potential energy curve cannot be constructed as the number

of dimensions (internal coordinates) is 3N-6 for a non-linear molecule of N-atoms. It is not surprising that the stable molecules are actually the stationary points of a graph of the reaction path. Stationary points with positive second derivatives (along the direction of the reaction path) correspond to observable chemical structures (intermediates, reactants, and products) because the coordinates represent a local energy minimum so that such molecules are stable; additionally, intermediate states are characterized with (or rather defined by) having higher energy than reactants and products. Transition states (TS), on the other hand, correspond to critical points along the reaction pathway with negative second derivative information; these structures are highly unstable and exist very briefly. Additionally, the van der Waals (VDW) structures are considered to be a local minimum along the reaction path between non-bonded chemicals which are physically attracted to one another. While not every reaction path has a VDW(s) structure that is easily distinguishable from the 'reactants' point, such VDW points always exist; this is out of necessity that no two chemical molecules can ever truly be infinitely distant from one another in any given reaction. The true 'reactant points' of chemicals in a reaction are defined as the sum of the electronic energy of each participating chemical molecule isolated from interaction with any other reactants. Mathematically, the positive second derivatives are merely positive eigenvalues of the hessian describing the coordinates; likewise, the TS point is at a saddle point with a single negative eigenvalue [24, Chater 12].

2.3   Transition State Confirmation

In searching for transition states, one typically can give a good guess of what the TS should look like. There are several clever methods that can be used that try to find the TS by the user providing the reactants and products as input data and the TS being interpolated [31][27, p. 616], one may also provide a guess for the TS additionally. From the experience of this research project, it is the opinion of the author that these methods are not very profitable except for very simple toy models. The best method for finding transition states, in the author's opinion, is to guess what the geometry of the TS looks like while fixing the distance between the atoms involved directly in the chemical reaction and optimising the geometry of the other atoms using the Hartree-Fock method. In practice the fixed bond length between the atoms directly involved in the chemical reaction has to be adjusted multiple times before finding a suitable distance; typically, the fixed bond length is anywhere between 1 and 3 Ångströms. After this initial optimisation, a full unconstrained (no fixed length) optimisation is performed using high level techniques such as density functional or perturbation methods. Finally, vibrational frequency analysis is

necessary to confirm that the reactants are in fact interacting in a manner to form (and/or break) a chemical bond. If a transition state is not found, then the guessed geometry's fixed lengths are adjusted and other bonds re-optimised until a suitable structure is identified. The molecular vibrations that are present in molecules can be described very accurately by the harmonic oscillator [24, Chapter 12]; for a one-dimensional harmonic oscillator the solution for the Schrödinger equation is:

$$\epsilon_{vib} = \left(\eta + \frac{1}{2}\right)h\upsilon : \eta \in 0, 1, \ldots \tag{2.17}$$

$$\upsilon = \frac{1}{2\pi}\sqrt{\frac{\kappa}{\mu}} \tag{2.18}$$

η is the quantum number (corresponding to a state), υ is the vibrational frequency, μ is the reduced mass, and κ is the force constant. From statistical mechanics we have the vibrational partition function given by:

$$q = \sum_{i=1}^{every\ state} \exp\left(-\frac{\epsilon_i}{k_bT}\right) \tag{2.19}$$

It follows easily, after plugging ϵ_{vib} into q, that for one mole:

$$q_{vib} = \frac{\exp\left(-\frac{h\upsilon}{2k_bT}\right)}{1 - \exp\left(-\frac{h\upsilon}{k_bT}\right)} \tag{2.20}$$

In the case of polyatomic molecules (of N atoms), one can think of many beads and springs or many harmonic oscillators; however, in this case, becomes a 3N-by-3N hessian matrix of coordinates [24, Chapter 12]. As mentioned before, we can diagonalise the hessian, these transformed coordinates are referred to as the vibrational normal coordinates. Here, if one eigenvalue is negative then the corresponding eigenvector vibrates along the direction of bond formation and the frequency is imaginary, observe υ. Finally, q_{vib} can be used to calculate the vibrational correction to the electronic energy.

2.4   Intrinsic Reaction Coordinates

After identifying all of the stationary points along the reaction pathway, one would like to know the reaction pathway itself; this is after all only a slice along the potential energy curve. The Intrinsic Reaction Coordinates are merely the points that connect the transition state to the other stationary points via method of steepest

descent on a mass-weighted coordinate path. This path is a differential equation [24, p. 344]:

$$\frac{d\mathbf{x}}{ds} = -\frac{g}{|g|} = v \tag{2.21}$$

$\mathbf{x}$ is defined as the mass-weighted coordinates, s is path length, v is the negative normalised gradient, g. Effectively, there are a number of numerical methods that can solve this equation; however, the default algorithm implemented by Gaussian '09 is the 'Hessian-based Predictor-Corrector integrator' method [21][22]. The HBPC method is a second-order iterative method which traces the IRC path by considering local information along each segment of the reaction path.

Chapter 3

Theoretical Study of a Pericyclic Reaction

In 1928, Otto Paul Hermann Diels and Kurt Alder reported the first known chemical pericyclic reaction to occur in a concerted manner between a diene and a 'dieneophile' [11]. Today primarily, the Diels-Alder reaction is defined by having a single transition state which is possible only because the double bonds of the diene are arranged in an s-cis formation so that 'electron pushing' is concerted. As a review, the s-cis geometry is characterised by the pair of double bonds positioned on the same side of the single bond connecting them. This 's-cis' geometric terminology should not be confused with the cis/trans assignment associated with the single bonds about the double bonds in question. Aside from these descriptions, there are no rigid rules for defining a Diels-Alder reaction, and it is because of the concerted push of electrons that there are no reaction intermediates. The first Diels-Alder reactions studied were between a conjugated diene and an alkene – the dieneophile – although in the research of this thesis the author assigned sulfur dioxide as the dienophile. In other words, the ring may be formed even by non-carbon elements.

The research herein, investigated the cheletropic addition of sulphur dioxide to 2,4 hexadiene using every technique discussed throughout this thesis within the environment of Gaussian '09 and GAMESS (The General Atomic and Molecular Electronic Structure System), the latter was used exclusively for molecular orbital localisation calculations to be discussed later in this thesis. The trans-trans isomer chemical reaction has been investigated to some extent previously using `B3LYP/6-311+G(d,p)`; here, however, the research includes every s-cis isomer: trans-trans, trans-cis, and cis-cis (respectively), as they each can react with sulfur dioxide:
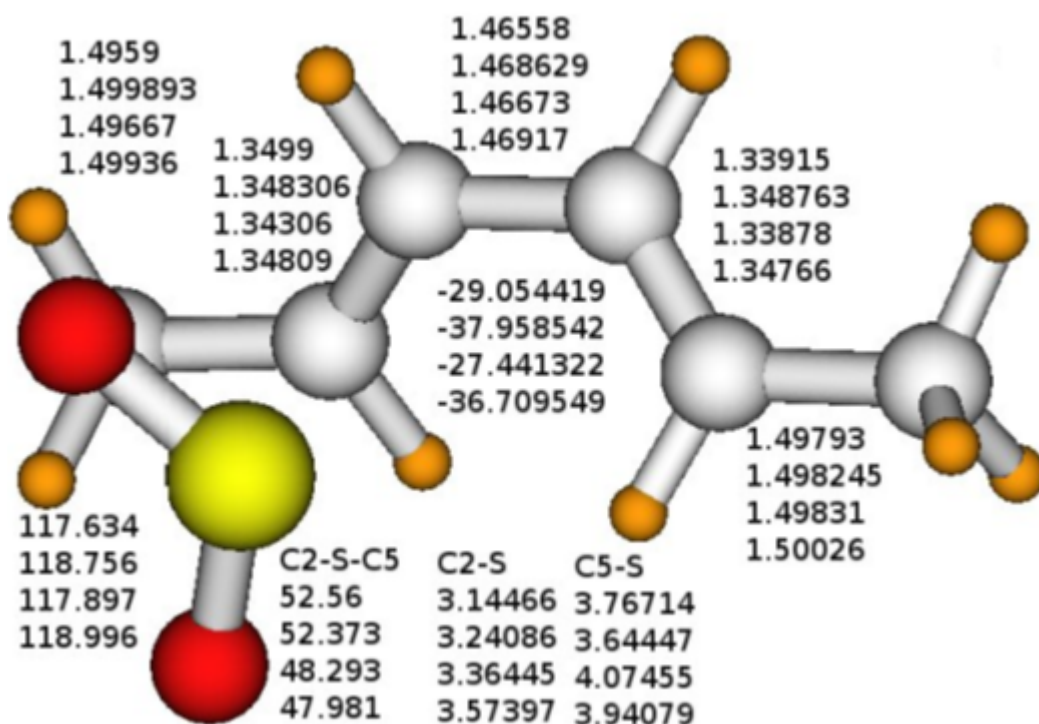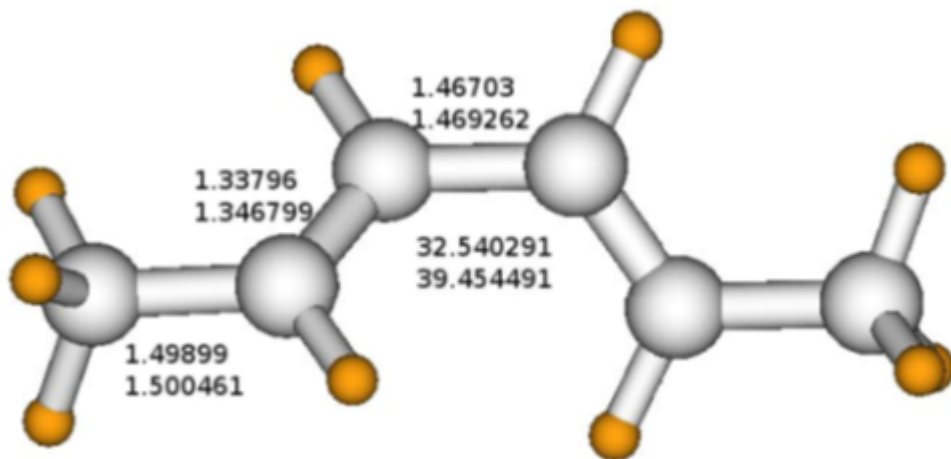
Figure 3.1: List of reactants
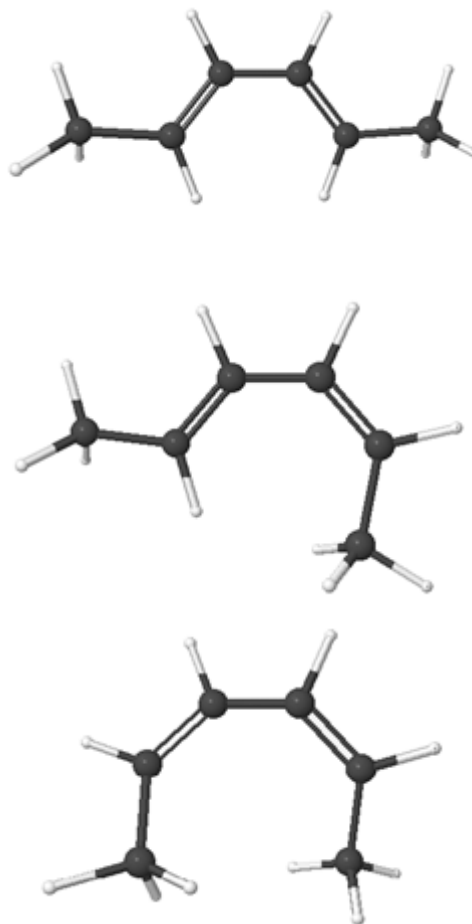
The reactions were investigated with a `6-311+G(d,p)` basis, at the level of B3LYP and MP2, with and without counterpoise correction to assess the effect of basis superposition error. To accurately present the geometry, in addition to reporting bond lengths, the author considered dihedral angles as a very good mark for revealing both reaction progression and comparing the accuracy of each method. The C2-C3-C4-C5 dihedral angle is monitored to show how 2,4-hexadiene contorts itself to get in phase for transition, it is here that symmetry is made and destroyed. On the other hand, the S-C2-C3-C4 dihedral is a good monitor of the alignment of the dienophile with the plane of the diene; additionally, it was interesting to monitor the subtle change in the SO_2 bond angle between various reactions and levels of theory.

Numerically, very tight convergence criteria and ultra-fine integration was used for all final optimisation calculations within the Gaussian '09 environment [1][3]; this is

merely the academic standard of imposing sufficiently strong conditions to get accurate results. Essentially, ultra-fine integration requires that the grid for numerical integration is very dense so that the measurement is 'almost continuous'. In the case of van der Waals structure calculations, special care was given to aide convergence and the QC (quadratically convergent) SCF procedure was implemented; essentially, linear searches are used when distant from optimisation and Newton-like steps when near except in the case of the energy increasing [3]. In general, this method should be avoided because it is very slow and usually unnecessary; however, in practice it was very robust.

In an attempt to preserve the highly symmetric nature of the (independent) diene, TS, and product, all VDW calculations were initialised from confirmed TSs with the dienophile pulled back until it was sufficiently distant from the reaction centre to prevent the formation of the product. In other words, many calculations were performed with sulfur dioxide initialised at various lengths from the reaction centre, in order to find the shortest distance such that sulfur dioxide would not converge in its geometry to a product. Special care was taken to ensure that the S-C2-C3 angle was equal to the S-C5-C4 angle as the dienophile was initialised at different distances. In the case of trans-trans and trans-cis, the dieneophile's position converged towards the side of the hexadiene's C1 atom. The reasons for this occurring in the case of the trans-cis molecule are quite clear from the unsymmetrical layout of the carbon atoms; however, the rationale for the trans-trans convergence is probably best understood as the convergent geometry being highly sensitive to initial conditions. Finally in the case of the cis-cis geometry, the VDW complex has the sulfur dioxide coordinated in closer proximity to the C5 atom than the C2 atom of the diene; this, too, is probably due to sensitivity to initial conditions. There are likely to exist many VDW complexes (for example with the dienophile behind the reaction centre, as opposed to in front of it), however only the VDW complex that is most likely to occur before a TS is formed is interesting for this study.

Although the author of this thesis does not believe that reaction schemes using arrows and harpoons are entirely accurate, due to the fact that such illustrations depict simple, idealistic movements of electrons as point particles, these schemes still provide some insight as they portray our best understanding of the progression of a chemical reaction in a naïve way. Here the reaction is summarised with such a mechanism:
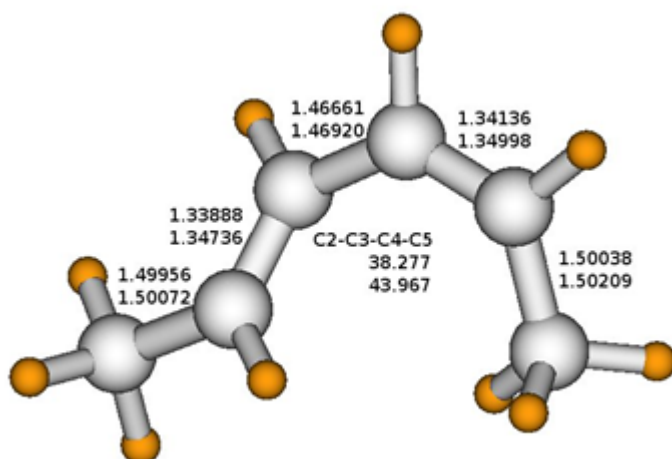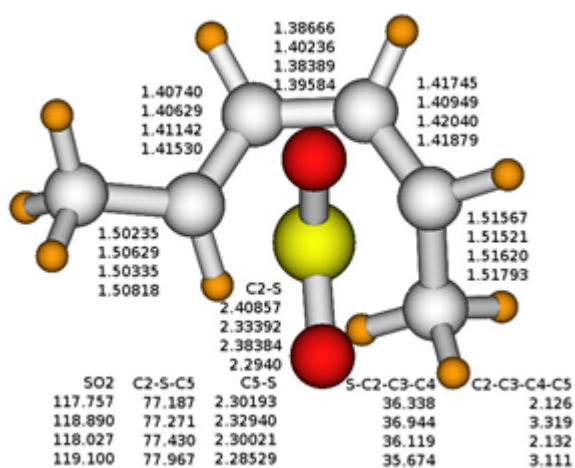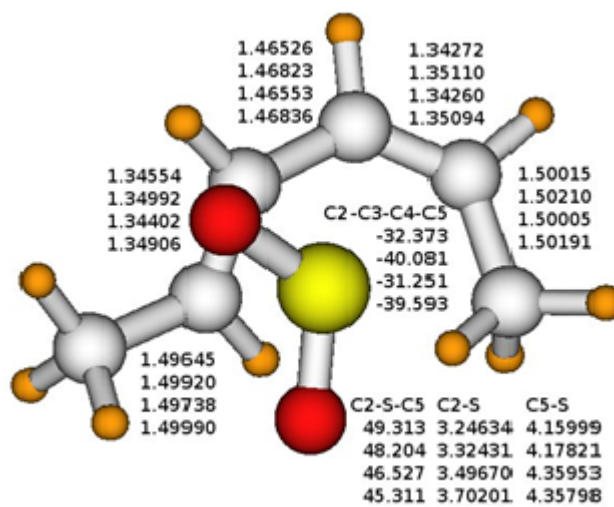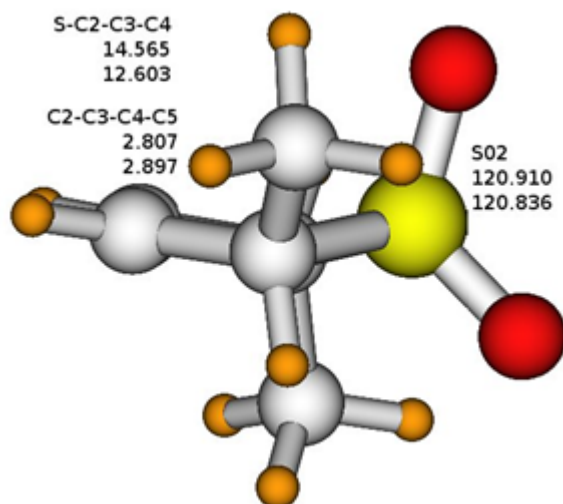
Figure 3.2: Proposed reaction mechanism

The reader should note that the oxygen atoms are actually intended to come in and out of the page with respect to the nearly planar 2,4-hexadiene. The striking feature of the first step in the mechanism is that all of the bond movement is heterolytic while standard literature on this mechanism depicts three homolytic movements. The author does not believe that the homolytic mechanism is more realistic because there is no reason that the lone pair of electrons on sulfur should prefer either double bond on the diene; nor is there any reason why a pair of electrons would want to attack the diene as a point-like pair. Additionally, the IRC calculations (below) strongly suggest a heterolytic mechanism. In any case, the electrons do not know that they move as half or full arrows. In fact, recent research by Karadakov *et al* also supports the heterolytic mechanism [20].

Returning to the discussion of geometry, in the illustrations below, all images list the C2-C3-C4-C5 dihedral angle within the ring structure; all values are listed in the following order, from top to bottom: B3LYP, CP-B3LYP, MP2, CP-MP2, except in the case where only two values are listed, B3LYP then MP2. Lengths, angles, and dihedrals are to be understood in context and thus explicit assignments are not shown when clear. If a value if completely omitted it is because of symmetry about the C3-C4 bond.

Figure 3.3: Illustrations of trans-trans reaction geometry progression

1.4959
1.499893
1.49667
1.49936

1.46558
1.468629
1.46673
1.46917

1.33915
1.348763
1.33878
1.34766

1.3499
1.348306
1.34306
1.34809

-29.054419
-37.958542
-27.441322
-36.709549

1.49793
1.498245
1.49831
1.50026

117.634
118.756
117.897
118.996

C2-S-C5	C2-S	C5-S
52.56	3.14466	3.76714
52.373	3.24086	3.64447
48.293	3.36445	4.07455
47.981	3.57397	3.94079

1.3845
1.39981
1.38101
1.39223

S-C2-C3-C4
39.862
40.877
39.133
39.088

1.41176
1.40731
1.41618
1.41771

0.000000
-0.000038
-0.000039
0.000047

1.50439
1.50637
1.50533
1.50848

S02
117.855
118.967
118.081
119.127

C2-S
1.46815
1.46125
1.46702
1.45738

C5-S
1.46987
1.46426
1.46916
1.4601

C2-S-C5
76.061
75.689
76.494
76.803

C2-C3-C4-C5
0.000004
0.000001
0.000023
0.000008

SO2
120.101
120.808
120.408
120.736

S-C2-C3-C4
11.250
14.265
10.680
12.942

19

The last two images are both showing the same product from two different angles, to illustrate more properties clearly. Furthermore, the isolated geometry of sulfur dioxide is only shown for comparison as it progresses throughout the chemical reaction. The key observations of the reaction are that the C2-C3-C4-C5 dihedral becomes planar during the transition state as it is as its product. Another striking feature is that the C2-C3 and C4-C5 bonds elongate as the reaction proceeds while the C3-C4 bond becomes progressively shorter. Additionally, the SO_2 bond angle becomes slightly wider in the product. Having shown the trans-trans geometry above, it is now appropriate to focus on the trans-cis reaction progression.

Figure 3.4: Illustrations of trans-cis reaction geometry progression

1.46526
1.46823
1.46553
1.46836

1.34272
1.35110
1.34260
1.35094

1.34554
1.34992
1.34402
1.34906

1.50015
1.50210
1.50005
1.50191

C2-C3-C4-C5
-32.373
-40.081
-31.251
-39.593

1.49645
1.49920
1.49738
1.49990

C2-S-C5	C2-S	C5-S
49.313	3.24634	4.15999
48.204	3.32431	4.17821
46.527	3.49670	4.35953
45.311	3.70201	4.35798

1.38666
1.40236
1.38389
1.39584

1.40740
1.40629
1.41142
1.41530

1.41745
1.40949
1.42040
1.41879

1.51567
1.51521
1.51620
1.51793

1.50235
1.50629
1.50335
1.50818

C2-S
2.40857
2.33392
2.38384
2.2940

SO2	C2-S-C5	C5-S	S-C2-C3-C4	C2-C3-C4-C5
117.757	77.187	2.30193	36.338	2.126
118.890	77.271	2.32940	36.944	3.319
118.027	77.430	2.30021	36.119	2.132
119.100	77.967	2.28529	35.674	3.111

21

Please, notice a distinct difference in geometry between the B3LYP (top) and MP2(bottom) calculations; further, observe the BSSE contribution has an unappreciable effect on geometry.
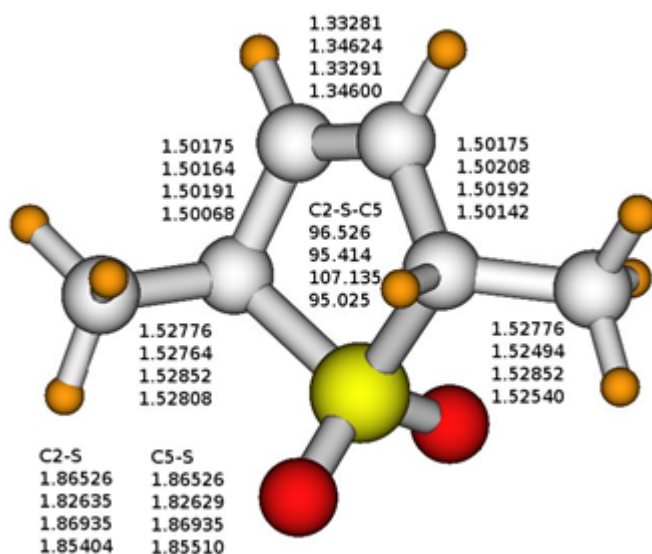
Very similar observations can be made about this reaction as well; the central dihedral angle becomes essentially planar at the transition state and the same bonds are either stretched or contracted appropriately. Finally, cis-cis reaction geometry progression is studied:

Figure 3.5: Illustrations of cis-cis reaction geometry progression

1.48196
1.47056
1.48196
1.47199

1.32491
1.34013
1.32491
1.34961

1.32737
1.34289
1.32737
1.35022

1.50265
1.49928
1.50265
1.50038

1.50208
1.49828
1.50208
1.49987

C2-S	C5-S	C2-C3-C4-C5	S-2-3-4	C2-S-C5	SO2
1.54832	3.22425	58.368	27.875	46.325	118.437
4.68980	3.53171	52.451	24.055	44.322	118.258
4.55034	3.29521	58.368	27.875	45.372	118.437
4.72361	3.72545	53.851	32.465	43.006	119.215

1.39288
1.39035
1.40663
1.40108

1.41019
1.4132
1.40991
1.41697

1.41032
1.41313
1.40649
1.41413

1.50742
1.50816
1.51147
1.51343

C2-S
2.44295
2.42907
2.39070
2.35631

C5-S
2.40890
2.40272
2.39093
2.35828

1.51217
1.51307
1.51543
1.51813

C2-C3-C4-C5	SO2	C2-S-C5	S-C2-C3-C4
2.019	117.623	79.306	33.933
1.886	117.961	79.346	33.971
3.972	118.745	79.560	33.073
3.234	119.092	79.854	32.589

Hopefully, it is evident that because the cis-cis and trans-trans isomers both undergo conrotatory ring closure, they both produce the same products (hence a redundant depiction of the identical product is omitted); however, the trans-cis isomer's ring closure occurs via a disrotatory mechanism.

As mentioned before, the geometry of a compound is intimately associated with its energy being minimised. However, it should be clear that there is not only one potential energy surface for each compound; it is the different basis sets and methods (variatonal or perturbation) which, in fact, give rise to different potential surfaces. Consequently, each surface will have different coordinate minimisers, and each minimum is only approaching the true Schrödinger energy surface; needless to say, a good method is one which has stationary points in an approximate neighbourhood of the actual wave-function's minimisers. To show this, one can compare improvements to methods (such as MP2 vs. MP3) and appreciate that the improvements

25

are convergent; in addition, independent methods (such as B3LYP vs MP2) which share similar data should give reassurance to our results. From our results above, it is seen that the biggest disagreements come with the cis-trans isomer; the VDW complex's C2-C3-C4-C5 dihedral has an array of values {-32.373, -40.081, -31.281, -39.593} over the techniques, which shows that the BSSE has a great impact on the validity of the results. However, it is noteworthy that the disagreement is not at the choice of method for solving the Schrödinger equation but whether or not CP correction is used, this should be no surprise as the molecules' wave-function should have significant overlap at this stage in the reaction mechanism. In contrast, the product's geometry is then affected not by BSSE but rather choice of method in the case of the S-C2-C3-C4 dihedral: B3LYP {-.669, -.629} and MP2 {12.603, 14.565}. Finally, a textbook example of the usefulness of CP correction is how the C2-S-C5 angle is more or less the same at the level of B3LYP {96.526 95.414} but how MP2 is corrected in correlation {107.135 95.025}. Clearly, each method has its strengths and weakness; only by comparing the geometry with the energy[1] can one begin to appreciate the reaction and gain some insight.

Table 3.1: Trans-Trans Isomer

All B3LYP energies relative to IRC calculated energy, -783.325657 Ha

All MP2 energies relative to IRC calculated energy, -781.673728 Ha

Reaction Point\Method	B3LYP	CP-B3LYP	MP2	CP-MP2
Reactants	-0.022616188	N/A	-0.019431270	N/A
VDW Complex	-0.029392055	-0.025822636	-0.029429152	-0.023788872
Transition State	0.000000457	0.008609926	0.000000135	0.017646206
Product	-0.028192148	-0.015122818	-0.036429410	-0.006620097

Table 3.2: Cis-Trans Isomer

All B3LYP energies relative to IRC calculated energy, -783.317404 Ha

All MP2 energies relative to IRC calculated energy, -781.667593 Ha

Reaction Point\Method	B3LYP	CP-B3LYP	MP2	CP-MP2
Reactants	-0.028392067	N/A	-0.023813548	N/A
VDW Complex	-0.034621519	-0.030914736	-0.033948875	-0.027676862
Transition State	-0.000927043	0.008253065	-0.000000432	0.018305898
Product	-0.035839507	-0.022923549	-0.042621174	-0.012721281

---

[1]Reported in Hartrees (Ha) 1 Ha = 4.35974394(22) $\times 10^{-18}$ J

Table 3.3: Cis-Cis Isomer

All B3LYP energies relative to IRC calculated energy, -783.304919 Ha

All MP2 energies relative to IRC calculated energy, -781.654075 Ha

Reaction Point\Method	B3LYP	CP-B3LYP	MP2	CP-MP2
Reactants	-0.03898957 19998776	N/A	0.03713861 41599714	N/A
VDW Complex	-0.04404162 09999057	-0.04090348 57209463	-0.04539448 43799263	-0.04000079 86310129
Transition State	0.00000671499 992677127	0.00947457 418408249	0.0000000865 900346980197	0.0184400 072730568

In the case of the B3LYP Trans,Trans-product, the final energy is lower than the reactant however not lower than the VDW, a similar trend exists for the CP-B3LYP and CP-MP2 calculation, only at the MP2 level (with BBSE) is product distinctly favourable. Likewise, in the Cis-Trans case the Counter-Poise correction methods brought the energy to be higher than the VDW complex while their analogue with BBSE continues to have lower energy compared with the VDW complex. In all calculations, the products with Counter-Poise correction are significantly higher than the reactants. In every case, the energy for the VDW complex is appreciably lower than the respective reactant's associated energy for the same level of theory, indicating that the complex is stable for reactants in solution.

The optimised single point transition states without a counter-poise correction were used as the starting point for the IRC calculations, the difference in energy illustrates to what order of magnitude the energy values can be trusted. Around the stationary points, the Berny algorithm[35][2] – and quasi-Newton methods in general – tend(s) to be oscillatory especially if the potential energy surface is particularly flat. Fortunately, the differences in energy are not particularly drastic; therefore, one can conclude that the various methods are strongly in agreement. Having presented the stationary geometry, it at least seems that the reaction would be concerted and follow the proposed heterolytic reaction mechanism; now the intrinsic reaction coordinates are studied which clearly demonstrates the proposed mechanism.

Trans-Trans IRC at level of B3LYP
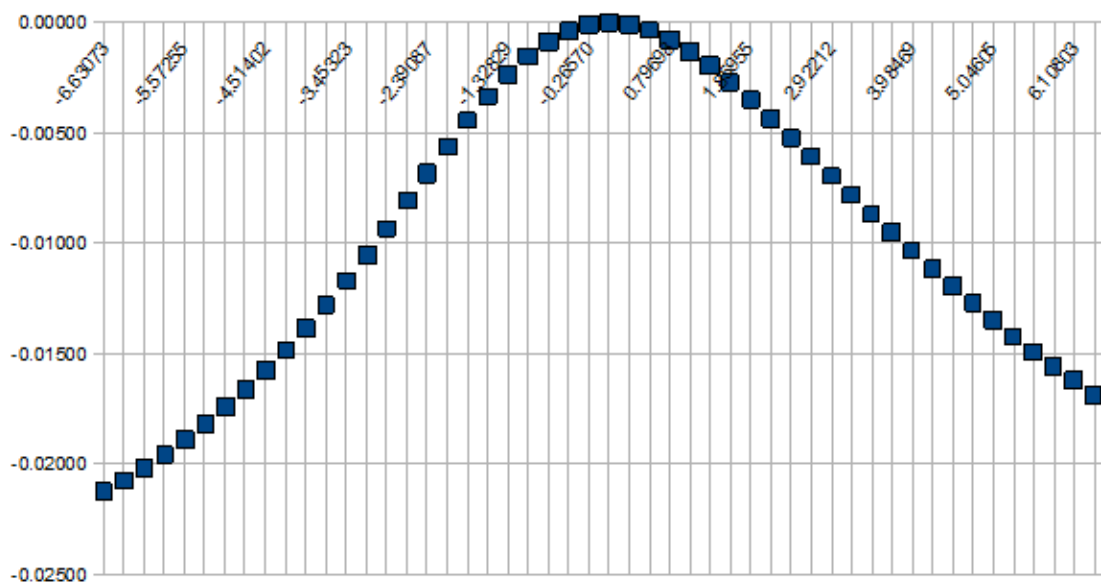
Trans-Trans IRC at MP2
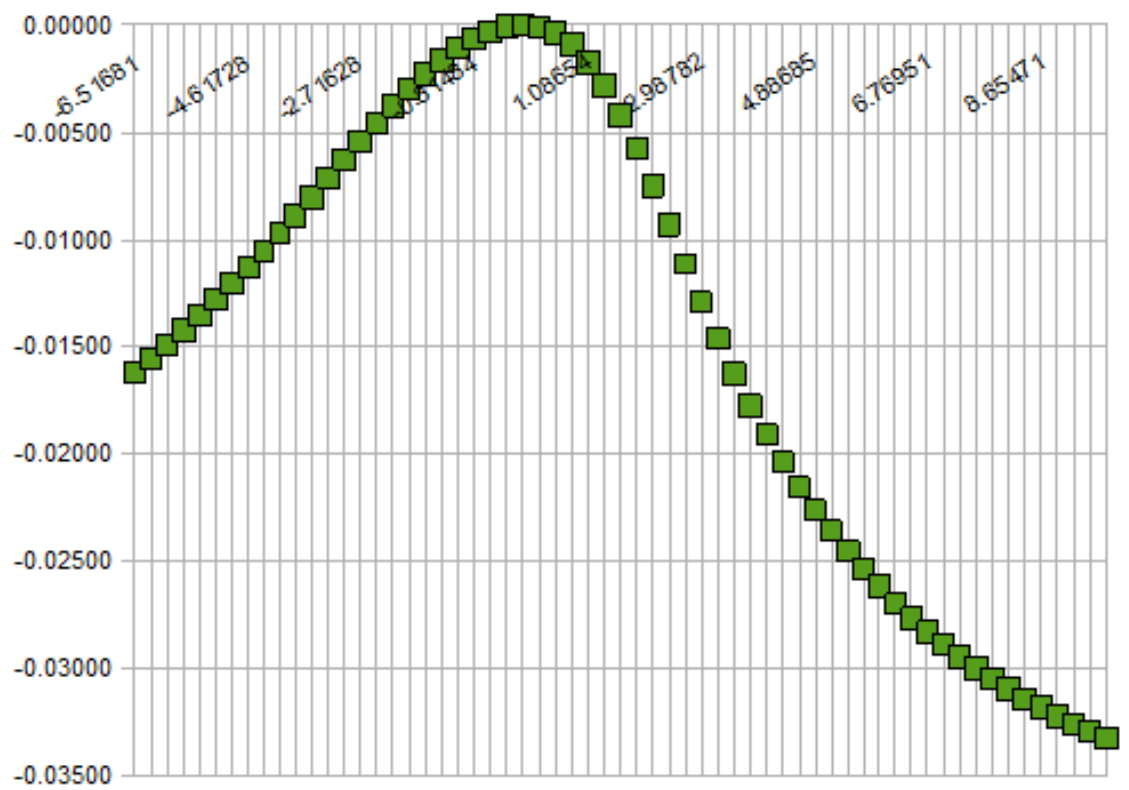
Cis-Trans IRC at B3LYP Level
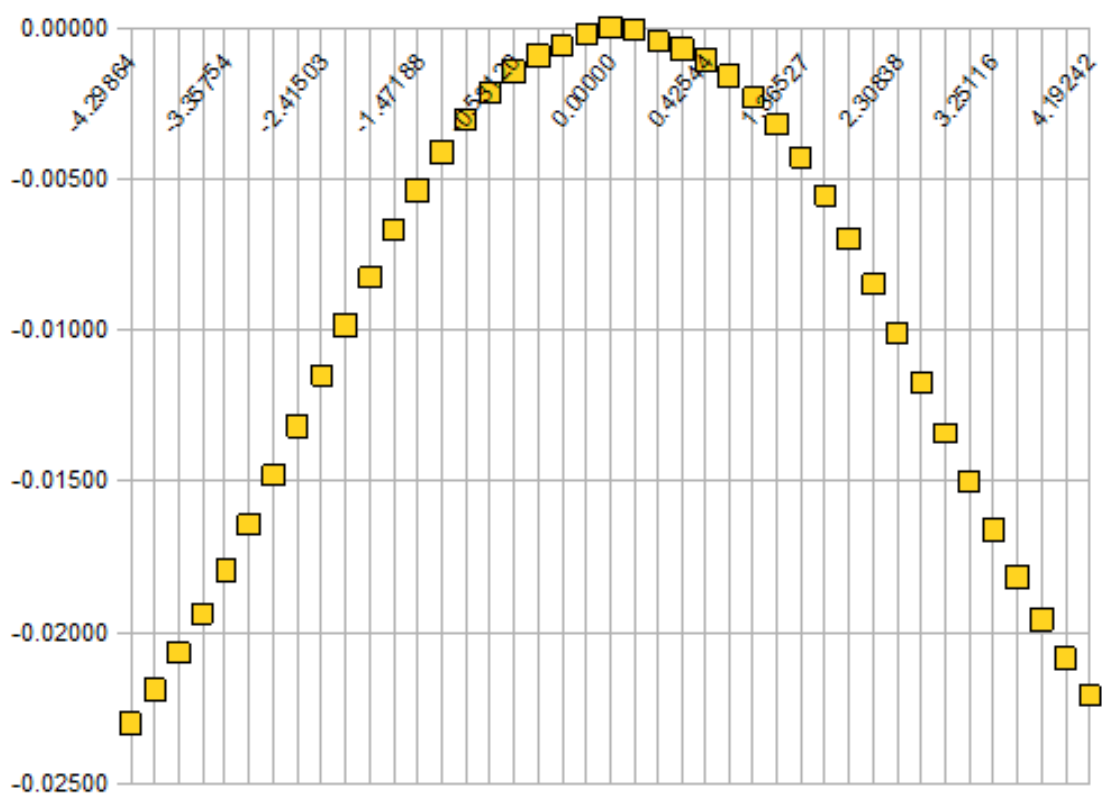
Cis-Trans IRC at MP2 Level

Cis Cis IRC at MP2 Level
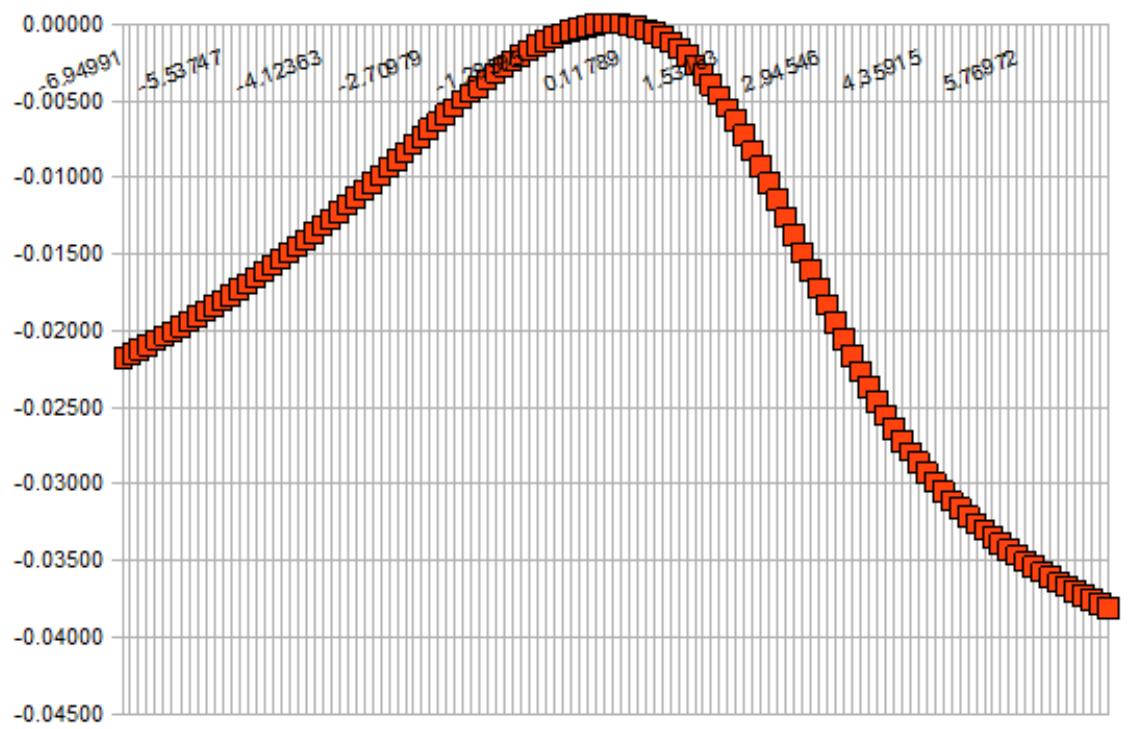
Cis Cis IRC at B3LYP Level
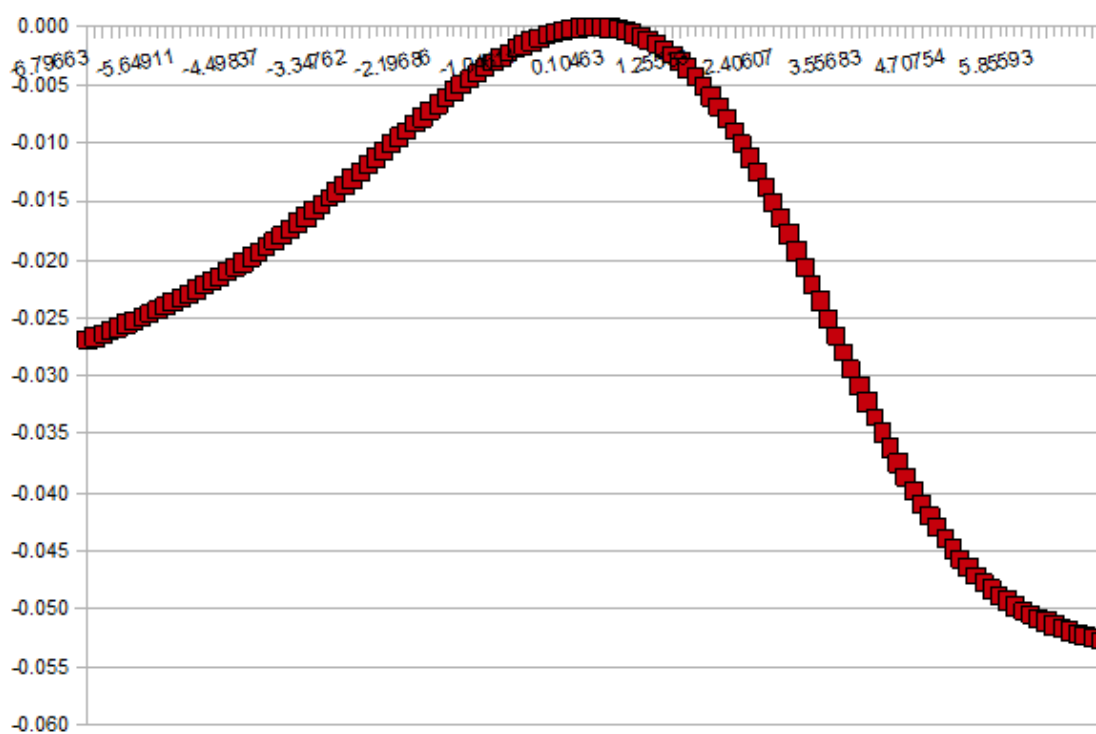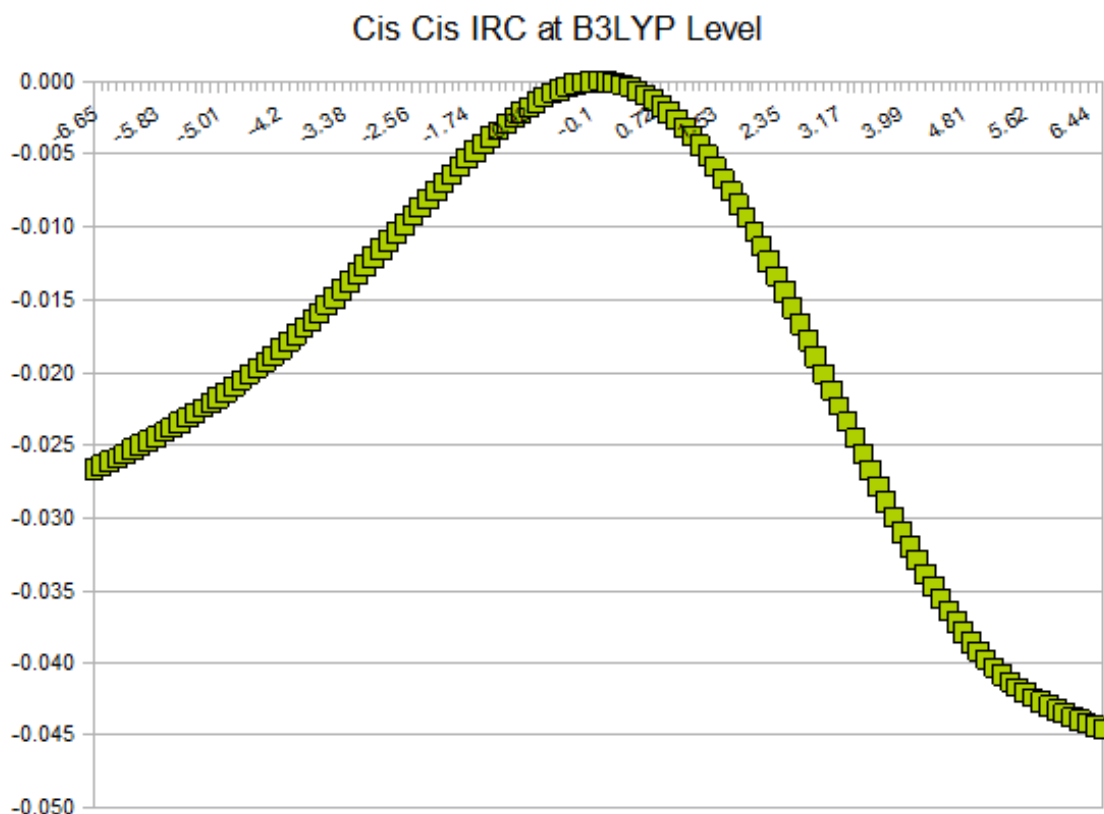
The IRC calculations confirm that the reaction is concerted, that is that there are no other hidden transition states or unanticipated intermediates. The MP2 calculations were taken further along the reaction coordinates to better approach the products or VDW complexes, to illustrate that the path connects these stationary points; while the B3LYP calculation was taken sufficiently far to confirm that the IRC starting point is the proper transition structure. The extraordinary number of points for the MP2 IRC calculations took less than 2 days each and it is the belief of the author that such calculations should be done if time and resources permit.

Before going into a detailed treatment of the theory of localised molecular orbitals and the various numerical methods for solving this quantum chemical problem (which is the emphasis for the remainder of this thesis), the author will first close this chapter on the investigation of the Diels-Alder reaction by simply presenting the hexadienes' localised molecular orbitals – which will provide a perfect segue for what is to come. By carefully analysing the localised molecular orbitals, one should be equipped to identify lone pairs of electrons, how molecular orbitals overlap to prepare for the transition state, and ultimately view a seamless transition to the product which comes naturally. The contour value is listed at the top left of every

33

image, this is a measure of the density of the molecular orbitals. Recall, that a normalised molecular orbital's wave-function exists over the entire domain yet chemists are ultimately only concerned with the behaviour of a wave-function in some reasonable neighbourhood of a chemical molecule. At its core, the localised molecular orbitals will provide us some insight in how the chemical bonds really behave. The localised molecular orbitals presented in this section are orthogonal – their associated molecular orbital overlap matrix is the identity matrix – as it will be shown in the following chapter, this is merely a mathematical convenience and there is no reason to assume that the actual molecular orbitals are orthogonal. Although this method is very limited, it is, to date, the soundest method for studying localised molecular orbitals. Clearly though, as it will be shown, the localised molecular orbitals have the advantage over canonical orbitals because their form – while not entirely localised – is at least not spread over entire parts of the molecule which is typical of the canonical form. Sulfur dioxide, in its free form, is presented as a basis of comparison, as it is surely far more well-known than the dienes studied.

The results show highly localised molecular orbitals and in the transition state it is clear where the bond formation is proceeding. As expected with the Pipek-Mezey method, the π and σ bonds are not separated very well, for example the Cis-Cis reactants HOMO; while the Edmiston-Rüdenberg and Boys methods show very similar results [32].

Table 3.4: SO_2 HOMO
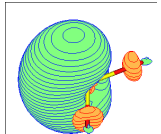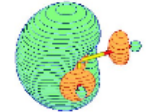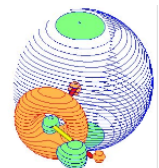
Edmiston-Rüdenberg	Boys	Pipek-Mezey
.05	.05	.1

Table 3.5: SO_2 LUMO
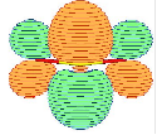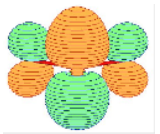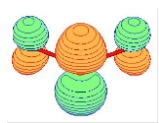
Edmiston-Rüdenberg	Boys	Pipek-Mezey
.05	.05	.01

Table 3.6: Trans-Trans HOMO
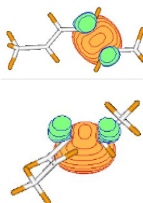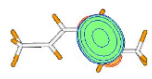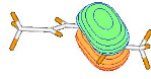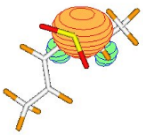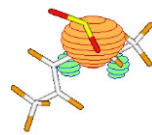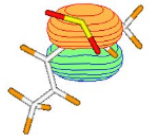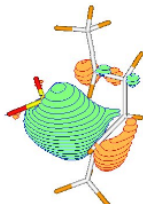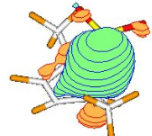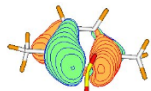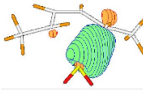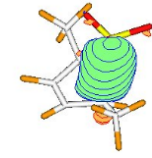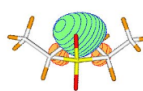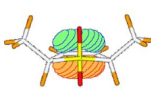
	Edmiston-Rüdenberg	Boys	Pipek-Mezey
2,4-hexadiene	.05	.05	.05
VDW complex	.05	.05	.05
Transition Structure	.05	.05	.05
	.075	.075	
Product	.05	1.0	1.0

Table 3.7: Trans-Trans LUMO
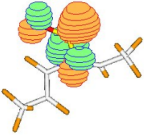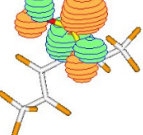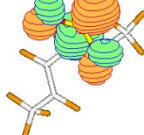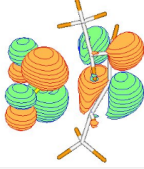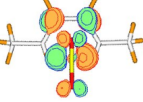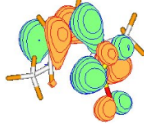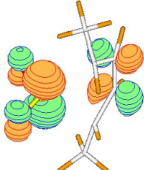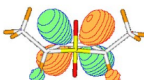
	Edmiston-Rüdenberg	Boys	Pipek-Mezey
2,4-hexadiene	.05	.05	.05
VDW complex	.05	.05	.05
Transition Structure	.05 <hr> .075	.075	.05 <hr> .05
Product	.05	.05	.05

Table 3.8: Cis-Trans HOMO
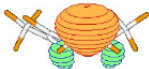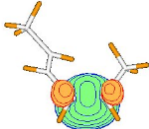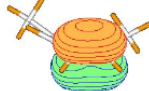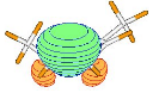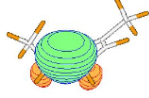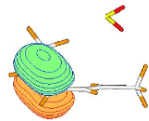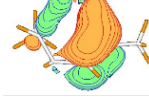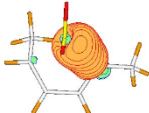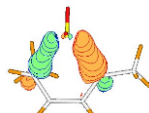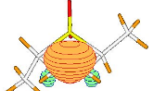
	Edmiston-Rüdenberg	Boys	Pipek-Mezey
2,4-hexadiene	.05	.05	.05
VDW complex	.05	.05	.05
Transition Structure	.05	.05	.05
	.075		.075
Product	.075	.075	.075

Table 3.9: Cis-Trans LUMO
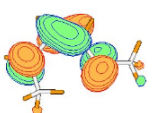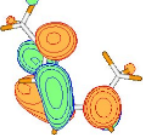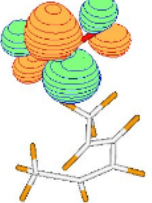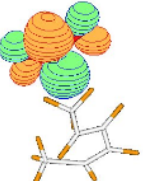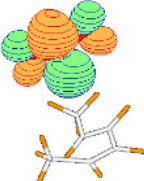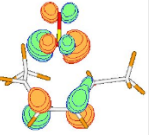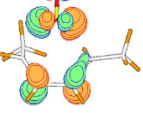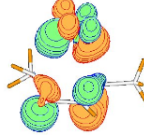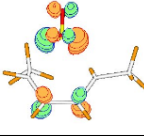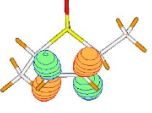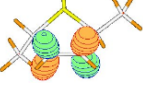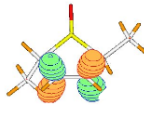
	Edmiston-Rüdenberg	Boys	Pipek-Mezey
2,4-hexadiene	.05	.05	.05
VDW complex	.05	.05	.05
Transition Structure	.075	.075	.05
			1.0
Product	.075	.075	.075

38

Table 3.10: Cis-Cis HOMO
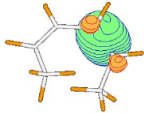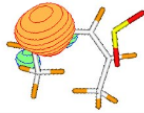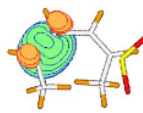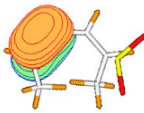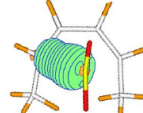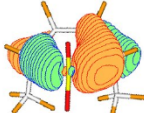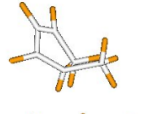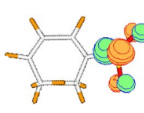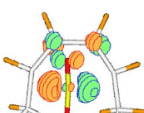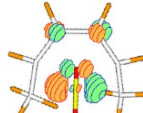
	Edmiston-Rüdenberg	Boys	Pipek-Mezey
2,4-hexadiene	.075	.075	.075
VDW complex	.05	.05	.05
Transition Structure	.1	.1	.05

Table 3.11: Cis-Cis LUMO

	Edmiston-Rüdenberg	Boys	Pipek-Mezey
2,4-hexadiene	.075	.075	.075
VDW complex	.05	.05	.05
Transition Structure	.1	.1	.05

39

Chapter 4

Localised Molecular Orbitals

As a review of quantum mechanics, all pertinent information of a particle – such as its energy, momentum, expectation value, etc. – is invariant under normalization of the wave-function (to see this simply re-solve the Schrödinger equation with the normalised form) :

$$\int_D |\psi|^2 \, d\tau = 1 \tag{4.1}$$

Essentially, this can be as an interpreted as 'the probability that a particle exists somewhere in the universe, D, is one' [34, Chapter 2]; similarly, in probability theory a probability distribution of many variables collectively summing to 1 is taken as an axiom. If a wave-function is not normalized, then it can easily be made as such by dividing by its magnitude. In many electron systems, the wave-functions exhibit properties very similar to classic waves, namely they can be interfering or constructive when interacting. Quantum chemists, who often deal with many such wave interactions, usually represent this property with a square matrix called the 'orbital overlap matrix' which is symmetric for real valued orbitals and for complex wave-functions the matrix is equal to its adjoint (complex conjugate transposed) [39, pp. 136-137]. The research of this thesis deals exclusively with real valued wave-functions when handling the subject of localised molecular orbitals; however, certain molecules, such as benzene, are modelled very well with complex form. The elements of the overlap matrix are every inner product of the wave functions:

$$[s]_{j,i} = \begin{pmatrix} \langle 1|1 \rangle & \langle 1|2 \rangle & \cdots & \langle 1|n \rangle \\ \langle 2|1 \rangle & \langle 2|2 \rangle & & \langle 2|n \rangle \\ \vdots & & \ddots & \vdots \\ \langle n|1 \rangle & \langle n|2 \rangle & \cdots & \langle n|n \rangle \end{pmatrix} = [s^*]_{i,j} \tag{4.2}$$

One consequence of the normalisation criteria of wave-functions is that concerning the overlap matrix, $S_{i,j}$, only diagonal elements, $s_{i,i}$, can be identically equal to one. In other words, off diagonal elements' magnitude must be less than one and greater or equal to zero [39, pp 136-137]. This follows immediately from the Cauchy-Schwarz inequality which formally says [4, Chapter 6]:

$$|\langle x|y\rangle|^2 \leq \langle x|x\rangle\langle y|y\rangle \tag{4.3}$$

$$\left|\sum_{i=1}^{n} x_i^* y_i\right|^2 \leq \sum_{j=1}^{n} |x_j|^2 \sum_{k=1}^{n} |y_k|^2 \tag{4.4}$$

Where the inner product is defined as:

$$\langle x|y\rangle = \int_D x^* y \, d\tau : x \in \mathbb{C}^n \tag{4.5}$$

As mentioned above, the normalization condition implies that the diagonal of the overlap matrix should be 1 for every element. If linear combinations of atomic orbitals (LCAO) are used to construct molecular orbitals[39, Chapter 3.4, pp. 136-137]:

$$\psi_j := \sum_{\mu=1}^{N} c_{j\mu} \chi_\mu \tag{4.6}$$

then the normalisation strategy is obvious:

$$\hat{\psi}_j := \sum_{\mu=1}^{N} \frac{c_{j\mu}}{\langle \chi_j|\chi_j\rangle^{1/2}} \chi \tag{4.7}$$

The normalisation condition is used because it keep the associated objective functions nicely bounded, simplifies the construction of the function, gradient, and hessian, and allows one to check that the overlap matrix is properly defined and that results make sense. Interestingly, it is somewhat difficult to understand what this definition really means because it is not immediately obvious that molecular orbitals – if they truly exist at all – should behave in such a linear fashion. Fortunately, in practice this method actually does accurately describe the molecular Schrodinger equation; the LCAO was first presented by John Lennard-Jones[26]. If one stores the mixing coefficients, $c_{j\mu}$, in an n-by-N matrix (with n denoting the number of atomic orbitals and N representing the number of molecular orbitals), the practice of fulfilling (4.7) is as simple as dividing every element of the jth row of the mixing coefficients by $\langle \psi_j|\psi_j\rangle^{1/2}$ then computing (4.6) once more. After applying the normalization criteria to the Cauchy-Schwarz inequality (4.3), it is very clear to see that the range of $s_{i,j}$ is from -1 to +1, with zero reserved for orthogonal molecular

orbitals. The irony of these assumptions, and why (4.4) is so important, is that in practice it has been observed that off diagonal elements may converge to +1, which should be used as a test to ensure that the methods used are working. Off diagonal elements equal to +1 imply that there is a linear dependence between the molecular orbitals which is clear from (4.3), in that the inner products are scalar multiples of one another. However, as it will be made very clear shortly this should never occur because the molecular orbitals are LCAO, and the combinations should be independent. Most often, in non-orthogonal MO-LCAO calculations, the basis is a the set of orthogonal MO-LCAO (which in turn is constructed from atomic orbitals) which translates to the overlap matrix being the identity matrix, to floating point precision; therefore only an ill linear combination could even get into such situations as off diagonal elements being ±1. Finally, another useful result is that the overlap matrix must be positive definite [7]; equivalently every real part of the eigenvalues must be greater than zero. We also have that the overlap matrix is in general Hermitian – if the inner product is taken over the real space then the overlap matrix reduces to a real symmetric matrix and – therefore the eigenvalues are positive. In practice it has been observed that the eigenvalues have been zero and off-diagonal elements equal to +1; this, in particular, has often been observed for optimisations taken using gradient-like methods, or when second-order methods converge to gradient-like methods.

One natural question is how to choose the coefficients $c_{j\chi}\chi$ of (4.6) in a manner that makes sense in an ordinary way; that is, how can one implement theoretical methods that stand the test of reality. Experience, of chemists, reveals that chemical bonds are experienced between near atoms – here avoid saying adjacent because such a statement would only be *ex post facto*, the chemical bonds *are precisely* the molecular orbitals to be defined – dense in the region of these atoms.

Returning to the case of wave-functions written as a single Slater determinant, it can be shown that the canonical MOs are invariant under unitary transformation (rotation):

$$\langle\psi_i|\psi_j\rangle = \delta_{ij} \tag{4.8}$$

$$\psi' = U\psi : UU^\dagger = I \tag{4.9}$$

$$\psi'_i = \sum_{i=1}^{n} u_{ij}\psi_j \tag{4.10}$$

$$\langle\psi'_i|\psi'_j\rangle = \langle U\psi_i|U\psi_j\rangle = \langle UU^\dagger\psi_i|\psi_j\rangle = \delta_{ij} \tag{4.11}$$

We emphasise that (4.6) and the above equations are equivalent for the current methods in constructing molecular orbitals; (4.6) is the problem of optimising molecular orbitals as a linear combination of atomic orbitals, while (4.9) is optimisation of molecular orbitals as linear combinations of other molecular orbitals which are

themselves linear combinations of molecular orbitals[25]. If one can solve (4.9), then each basis molecular orbital can be presented by transforming it back to atomic orbitals given the inverse transformation of the transformation that converted the AOs to MOs in the first place.

Many times, the aim of localised molecular orbitals is to find solutions which are consistent among functional groups between unrelated chemical compounds. For example, the ester group ($RC[=O]OR'$) should have similar looking MOs regardless of what it is connected to, if its MO's are truly localised. A set of LMOs is usually defined by optimising the expectation value of a two-electron operator [32]

$$\langle \Omega \rangle = \sum_{i=1}^{n} \langle \psi_i' \psi_i' | \Omega | \psi_i' \psi_i' \rangle \tag{4.12}$$

Currently, this equation is solved by successive series of orbital rotations; and the choice of Ω need not be unique. There are various methods, in our research we used Edmiston-Ruedenberg, Pipek-Mezey, and Boys methods for solving the localised molecular orbital problem. The Boys method uses the square of the difference between two electrons for Ω:

$$\langle \Omega \rangle_{Boys} = \sum_{i=1}^{n} \langle \psi_i' \psi_i' | (r_1 - r_2)^2 | \psi_i' \psi_i' \rangle \tag{4.13}$$

This is perhaps the most intuitive of the methods because it aims to minimise the spatial occupation of the molecular orbitals; highly spatially compact MOs are comparable to our ideal chemical bond between adjacent atoms. It can also be shown that the minimisation of Boys method is equivalent to maximising:

$$\langle \Omega \rangle_{Boys}' = \frac{1}{2} \sum_{i=1}^{n} \sum_{j=1}^{n} \left(\frac{\langle \psi_i' | r | \psi_i' \rangle}{\langle \psi_i' | \psi_i' \rangle} - \frac{\langle \psi_j' | r | \psi_j' \rangle}{\langle \psi_j' | \psi_j' \rangle} \right)^2 \tag{4.14}$$

This representation is not arbitrary, the terms $\frac{\langle \psi_i' | r | \psi_i' \rangle}{\langle \psi_i' | \psi_i' \rangle}$ are referred to the centroids of the orbitals and maximising these is intuitively (and mathematically) equal to minimising their occupation. Further the calculations are made easier by the fact that the functions are not directly handled but rather their inner products are manipulated so that the operations reduce to straightforward matrix algebra. The single electron integrals (inner products) of the molecular orbitals are taken from their associated atomic orbital integrals:

$$\langle \psi_i | r | \psi_j \rangle = \sum_{\alpha}^{N} c_{\alpha i} \left(\sum_{\beta}^{N} c_{\beta j} \langle \chi_\alpha | r | \chi_\beta \rangle \right) \tag{4.15}$$

43

Then the problem of optimising the localised molecular orbitals is solved essentially by finding the best linear combination of single electron integrals (the basis). The exact algorithm for carrying out the optimisation is fairly straightforward and typical computations

take anywhere between 5 to 10 minutes. Given two molecular orbitals, $\{\psi_i, \psi_j\}$, Boys' procedure constructs a new pair via a two dimensional unitary transformation [32]:

$$\begin{pmatrix} \psi_i' \\ \psi_j' \end{pmatrix} = \begin{pmatrix} \cos\zeta & \sin\zeta \\ -\sin\zeta & \cos\zeta \end{pmatrix} \begin{pmatrix} \psi_i \\ \psi_j \end{pmatrix} \tag{4.16}$$

These rotations are performed pair wise until the objective function converges and the elements of the transformation matrix are arbitrarily close between successive iterations. The Edmiston-Ruedenberg (ER) localisation method, on the other hand, aims to maximise the inverse of the distance between the electrons [24, 9.4]:

$$\langle\Omega\rangle_{ER} = \sum_{i=1}^{n} \left\langle \psi_i'\psi_i' \left| \frac{1}{|r_1 - r_2|} \right| \psi_i'\psi_i' \right\rangle \tag{4.17}$$

It is often said that this corresponds to maximisation of self-repulsion energy, but notably this method and Boys both utilise a power of the distance between electrons. The Pipek-Mezey localisation method is the unintuitive method, in that it does not aim to optimise distances associated with electrons but rather attempts to maximise the sum the Mulliken atomic charges. In some, indirect, manner this will also solve the LMO spatial problem but it is not immediately obvious [24, 9.4]:

$$\langle\Omega\rangle_{PM} = \sum_{A=1}^{Atoms} [\rho_i(A)]^2 \tag{4.18}$$

$$\rho_i(A) = \sum_{\alpha \in A}^{AO} \sum_{\beta \in A}^{AO} c_{\alpha i} c_{\beta i} S_{\alpha\beta} \tag{4.19}$$

Calculations associated with this technique give rise to σ/π-bond separation which is popular among organic chemists, while Boys and Edmiston-Ruedenberg methods do not preserve this property [32].

Often orthogonal localized molecular orbitals are in fact delocalized more than one should desire simply because after computing the second derivatives of these functions it is found that the solution is not optimised. Since these optimised solutions correspond to localised molecular orbitals, it is obvious that the molecular orbitals are simply not localised to their limits unless an optimum solution is found to these equations. Ideally, one would like a solution which is global, so that the solution

set could have no further improvement; this would give us much insight. Clearly, every theory has its limit and the fact that there are multiple equations alludes to the obvious, that chemical bonding is a highly complex process; if a global solution were available one could visualise molecular orbitals as best as they could be given a particular set of equations. A global minimiser, $x^\diamond$, is one such that [12, Chapter 2]:

$$f(x^\diamond) \leq f(y) : \forall y \in \mathbb{R}^n \tag{4.20}$$

While a local minimum is a solution, $x^\star$, such that under a restricted neighbourhood $D^n \subset \mathbb{R}^n$, the above equation is true for all points in the neighbourhood. The theme of this entire thesis – more or less – is the subject of numerical solutions where the problem is 'chemical' and the coordinates are atoms or molecular orbitals; formal quantum mechanics is only our 'rule book' which motivates our mathematical methods. Because most physical problems have a massive number of local solutions, over their entire domain, it is generally the case that global solutions are impossible to find; however, there is a rich theory of research devoted to this problem. In our research, however, we are concerned principally on finding local solutions; in the case of the Boy's problem, for example, a local solution is very non-trivial and would be highly valued regardless if it is global. A local solution has a few requirements [12, Chapter 2]:

1. Every dimension of the function must collectively either be positive or negative in concavity; because positive concavity corresponds to function minimisers and negative concavity corresponds to function maximisers, it would make no sense to talk about a local solution existing with parts being minimisers and others being maximisers (one optimises functions as a whole and not *only* their individual dimensions). The exception to this case is many constrained optimisations and finding a transition state, these correspond to saddle point algorithms.

2. However, one must optimise each individual dimension after a function has dimensions with all the same concavity. At this point, it is clear that if each dimension can be optimised further (while maintaining dimensions of consistent concavity) then they simply should be. At this point, it is appropriate to consider the coordinate to be near a local solution and many simple, fast techniques are used, such as the ordinary Newton-Raphson iterative scheme which has quadratic convergence. Each dimension is converged when the norm of the gradient is small (each dimension's associated slope is approaching zero).

3. The solution should be locally smooth; in other words, the function isn't hyperactive in the neighbourhood of a solution. If this were the case, if might be that one were detecting a dent on a 'hill' towards the solution, rather than the solution itself. It might seem very abstract to even bother with the definition

of continuity one would find in analysis texts:

$$\forall \epsilon > 0 \quad \exists \delta > 0 \quad s.t. \quad |x - y| < \delta \Rightarrow |f(x) - f(y)| < \epsilon \tag{4.21}$$

However, this is has a perfectly natural interpretation in the computational optimisation setting; namely, if a numerical method moves the coordinates slightly then the function value should also only slightly when the objective function is convergent, assuming the other criteria is met.

Returning to the case of the Boys function, we realise that in practice the solution coordinates do not satisfy the first condition above, even though they are convergent under pair-wise rotations with respect to the objective function. If one were to relax the condition that the transformed molecular orbitals necessarily be constructed orthogonal to one another, then an unconstrained optimisation of these functions can be attempted; one should also expect that the orthogonal localised molecular orbital solutions are a good start for finding solutions to the non-orthogonal LMOs (NOLMOs) problem. There are a number of numerical methods which employ second derivative information; here a discussion of the methods studied is covered. In order to find a local optimised solution for the Boy's problem, first and second derivative information must be known; here is presented the analytical derivations for these derivatives as lucid as possible.

The following short-hand — $\psi_i = i$ and $\frac{\langle \acute{i}|r|\acute{i}\rangle}{\langle \acute{i}|\acute{i}\rangle} = [\acute{i}_r]$ — will be used in order to keep the derivations neat, compact, and succinct. Additionally, over the real valued space of wave-functions, it is apparent that $\frac{\partial \langle \acute{i}|r|\acute{i}\rangle}{\partial c_{xy}} = \delta_{ix}(\langle \acute{i}|r|y\rangle + \langle y|r|\acute{i}\rangle) = \delta_{ix}2\langle \acute{i}|r|y\rangle$, where the bra and ket components can be switched freely after applying the chain rule; likewise, $\frac{\partial \langle \acute{i}|\acute{i}\rangle}{\partial c_{xy}} = \delta_{ix}2\langle \acute{i}|y\rangle$.

$$B = \frac{1}{2}\sum_{i=1}^{n}\sum_{j=1}^{n}([\acute{i}_r] - [\acute{j}_r])^2 \tag{4.22}$$

$$\frac{\partial B}{\partial c_{pq}} = \frac{1}{2}\left\{\sum_{i=1}^{n}\delta_{ip}\frac{\partial\left(\sum_{j\neq p}^{n}([\acute{i}_r] - [\acute{j}_r])^2\right)}{\partial c_{pq}} + \sum_{i\neq p}^{n}\frac{\partial\left(\sum_{j=1}^{n}\delta_{jp}([\acute{i}_r] - [\acute{j}_r])^2\right)}{\partial c_{pq}}\right\}$$

$$\frac{\partial B}{\partial c_{pq}} = \frac{1}{2}\left\{\frac{\partial\left(\sum_{j=1}^{n}([\acute{p}_r] - [\acute{j}_r])^2\right)}{\partial c_{pq}} + \frac{\partial\left(\sum_{i=1}^{n}([\acute{i}_r] - [\acute{p}_r])^2\right)}{\partial c_{pq}}\right\}$$

$$\frac{\partial B}{\partial c_{pq}} = \frac{1}{2}\left\{2\sum_{j=1}^{n}([\acute{p}_r] - [\acute{j}_r])\frac{\partial[\acute{p}_r]}{\partial c_{pq}} + 2\sum_{i=1}^{n}([\acute{i}_r] - [\acute{p}_r])\frac{\partial(-[\acute{p}_r])}{\partial c_{pq}}\right\}$$

By symmetry,

$$\frac{\partial B}{\partial c_{pq}} = 2 \sum_{i=1}^{n} ([\acute{p}_r] - [\acute{i}_r]) \frac{\partial [\acute{p}_r]}{\partial c_{pq}}$$

$$\frac{\partial [\acute{p}_r]}{\partial c_{pq}} = 2 \frac{\langle \acute{p}|\acute{p}\rangle \langle \acute{p}|r|q\rangle - \langle \acute{p}|q\rangle \langle \acute{p}|r|\acute{p}\rangle}{\langle \acute{p}|\acute{p}\rangle^2} = 2(\langle \acute{p}|r|q\rangle - \langle \acute{p}|q\rangle \langle \acute{p}|r|\acute{p}\rangle)$$

$$\frac{\partial B}{\partial c_{pq}} = 4(\langle \acute{p}|r|q\rangle - \langle \acute{p}|q\rangle \langle \acute{p}|r|\acute{p}\rangle) \sum_{i=1}^{n} ([\acute{p}_r] - [\acute{i}_r]) \tag{4.23}$$

This completes the derivation of the first derivative, where the normalisation condition is used insofar as it simplifies the results; however, it is necessary to keep normed terms when computing the second derivative (such as $\langle i|i\rangle$) because they are functionals that change with respect to the mixing coefficients. Finally, it is noted that in practice $\sum_{i=1}^{n}([\acute{p}_r] - [\acute{i}_r]) = n[\acute{p}_r] - \sum_{i=1}^{n}[\acute{i}_r]$.

$$\frac{\partial^2 B}{\partial c_{st} \partial c_{pq}} = 2 \left\{ \frac{\partial \left[\frac{\partial [\acute{p}_r]}{\partial c_{pq}} \right]}{\partial c_{st}} \sum_{i=1}^{n} ([\acute{p}_r] - [\acute{i}_r]) + \frac{\partial [\acute{p}_r]}{\partial c_{pq}} \frac{\partial \sum_{i=1}^{n} ([\acute{p}_r] - [\acute{i}_r])}{\partial c_{st}} \right\}$$

$$\frac{\partial \sum_{i=1}^{n} ([\acute{p}_r] - [\acute{i}_r])}{\partial c_{st}} = (n-1) \frac{\partial [\acute{s}_r]}{\partial c_{st}} \delta_{ps} - \frac{\partial [\acute{s}_r]}{\partial c_{st}} (1 - \delta_{ps})$$

$$\frac{\partial^2 [\acute{p}_r]}{\partial c_{st} \partial c_{pq}} = \delta_{ps} \left\{ \frac{\partial \left[\frac{2}{\langle \acute{p}|\acute{p}\rangle^2} (\langle \acute{p}|\acute{p}\rangle \langle \acute{p}|r|q\rangle - \langle \acute{p}|q\rangle \langle \acute{p}|r|\acute{p}\rangle) \right]}{\partial c_{st}} \right\}$$

$$= 2 \left(\frac{1}{\langle \acute{p}|\acute{p}\rangle^2} \frac{\partial [\langle \acute{p}|\acute{p}\rangle \langle \acute{p}|r|q\rangle - \langle \acute{p}|q\rangle \langle \acute{p}|r|\acute{p}\rangle]}{\partial c_{st}} + (\langle \acute{p}|\acute{p}\rangle \langle \acute{p}|r|q\rangle - \langle \acute{p}|q\rangle \langle \acute{p}|r|\acute{p}\rangle) \frac{\partial \langle \acute{p}|\acute{p}\rangle^{-2}}{\partial c_{st}} \right)$$

$$\text{where } \tfrac{\partial \langle \acute{p}|\acute{p}\rangle^{-2}}{\partial c_{st}} = -2\langle \acute{p}|\acute{p}\rangle^{-3} 2\langle \acute{p}|t\rangle \delta_{ps} = -4\langle \acute{p}|t\rangle \delta_{ps}$$

$$= 2\delta_{ps} \left\{ \left(2\langle \acute{p}|t\rangle \langle \acute{p}|r|q\rangle + \langle t|r|q\rangle - 2\langle \acute{p}|q\rangle \langle \acute{p}|r|t\rangle - \langle t|q\rangle \langle \acute{p}|r|\acute{p}\rangle \right) - 4\langle \acute{p}|t\rangle (\langle \acute{p}|r|q\rangle - \langle \acute{p}|q\rangle \langle \acute{p}|r|\acute{p}\rangle) \right\}$$

If these parts are carefully combined,

$$\frac{\partial^2 [\acute{p}_r]}{\partial c_{st} \partial c_{pq}} = 2\delta_{ps} \left\{ -2\big(\langle \acute{p}|t\rangle\langle \acute{p}|r|q\rangle + \langle \acute{p}|q\rangle\langle \acute{p}|r|t\rangle\big) + \langle t|r|q\rangle - \langle t|q\rangle\langle \acute{p}|r|\acute{p}\rangle + 4\langle \acute{p}|t\rangle\langle \acute{p}|q\rangle\langle \acute{p}|r|\acute{p}\rangle \right\}$$

which is obviously symmetric with respect to second derivatives (interchanging t and q).

If we consider each case, $\delta_{ps} = \{0, 1\}$, separately then the symmetry of the second derivatives of the Boy's function should be more clear.

$$\frac{\partial^2 B}{\partial c_{st} \partial c_{pq}} = -8(\langle \acute{p}|r|q\rangle - \langle \acute{p}|q\rangle\langle \acute{p}|r|\acute{p}\rangle)(\langle \acute{s}|r|t\rangle - \langle \acute{s}|t\rangle\langle \acute{s}|r|\acute{s}\rangle) : \text{if } s \neq p \qquad (4.24)$$

Obviously this is symmetric, if one were to switch the q and t terms the second derivative is preserved. If $s = p$:

$$\frac{\partial^2 B}{\partial c_{st} \partial c_{pq}} = 2 \left\{ \frac{\partial^2 [\acute{p}_r]}{\partial c_{st} \partial c_{pq}} \left(n[\acute{p}_r] - \sum_{i=1}^{n} [\acute{i}_r] \right) + \frac{\partial [\acute{p}_r]}{\partial c_{pq}} (n-1) \frac{\partial [\acute{s}_r]}{\partial c_{st}} \right\} \qquad (4.25)$$

$$\frac{\partial^2 B}{\partial c_{st} \partial c_{pq}} = 4 \left[\left\{ -2(\langle \acute{p}|t\rangle\langle \acute{p}|r|q\rangle + \langle \acute{p}|q\rangle\langle \acute{p}|r|t\rangle) + \langle t|r|q\rangle - \langle t|q\rangle\langle \acute{p}|r|\acute{p}\rangle + 4\langle \acute{p}|t\rangle\langle \acute{p}|q\rangle\langle \acute{p}|r|\acute{p}\rangle \right\} \times \right.$$
$$\left. \left(n\langle \acute{p}|r|\acute{p}\rangle - \sum_{i=1}^{n} \langle \acute{i}|r|\acute{i}\rangle \right) + (\langle \acute{p}|r|q\rangle - \langle \acute{p}|q\rangle\langle \acute{p}|r|\acute{p}\rangle)(2n - 2)(\langle \acute{s}|r|t\rangle - \langle \acute{s}|t\rangle\langle \acute{s}|r|\acute{s}\rangle) \right]$$
$$(4.26)$$

There is a convenient representation for these somewhat messy equations, using matrices it becomes apparent that all the terms above can easily be called (within the environment of FORTRAN or MATLAB, for example) and used for computing. If one lets $\langle I|J\rangle$ represent the overlap matrix for the atomic orbitals, then taking linear combinations of the elements of this matrix one can represent all of the necessary elements. Here subscripts are used to indicate the dimensions to avoid ambiguity.

$$C * \langle I|J\rangle = \begin{pmatrix} c_{11} & \cdots & c_{1N} \\ \vdots & & \vdots \\ c_{n1} & \cdots & c_{nN} \end{pmatrix}_{n \times N} \begin{pmatrix} \langle 1|1\rangle & \cdots & \langle 1|N\rangle \\ \vdots & & \vdots \\ \langle N|1\rangle & \cdots & \langle N|N\rangle \end{pmatrix}_{N \times N}$$
$$= \begin{pmatrix} \langle 1'|1\rangle & \cdots & \langle 1'|N\rangle \\ \vdots & & \vdots \\ \langle n'|1\rangle & \cdots & \langle n'|N\rangle \end{pmatrix}_{n \times N} = \langle I'|J\rangle \qquad (4.27)$$

$$C * \langle I'|J \rangle^T = \begin{pmatrix} c_{11} & \cdots & c_{1N} \\ \vdots & & \vdots \\ c_{n1} & \cdots & c_{nN} \end{pmatrix}_{n \times N} \begin{pmatrix} \langle 1'|1 \rangle & \cdots & \langle n'|1 \rangle \\ \vdots & & \vdots \\ \langle 1'|N \rangle & \cdots & \langle n'|N \rangle \end{pmatrix}_{N \times n}$$

$$= \begin{pmatrix} \langle 1'|1' \rangle & \cdots & \langle n'|1' \rangle \\ \vdots & & \vdots \\ \langle 1'|n' \rangle & \cdots & \langle n'|n' \rangle \end{pmatrix}_{n \times n} = \langle I'|J' \rangle \qquad (4.28)$$

$$\text{provided } \sum_{\mu=1}^{n} c_{j\mu} \langle i|\mu \rangle = \langle i|j' \rangle$$

To get the position values, $\langle \acute{i}|r|\acute{j} \rangle$, the same method is applied to the matrix $\langle I|r|J \rangle$. The matrices above represent the traditional orthogonal localised molecular orbitals; so that the OLMO overlap matrix $\langle I'|J' \rangle$ is identity. Appropriately, one can use a similar set of OLMO mixing coefficients, $D_{n \times n}$, to construct the NO-LMOs which optimally solve the Boys function. In summary:

$$\phi_i = \sum_{j=1}^{n} d_{ij} \psi_j = \sum_{j=1}^{n} d_{ij} \sum_{k=1}^{N} c_{jk} \chi_k \quad \forall i \qquad (4.29)$$

Once the final optimisation is complete, the matrix product of D and C will represent how to mix the atomic orbitals – in the form of one electron integrals – best. Practically, one can simplify the Boys problem even further through choosing to make the non-orthogonal localised molecular orbitals constructed as 'unit self-contribution' plus a linear combination of the other orbitals, over each iteration, k, of the calculation:

$$(\phi_i)_k = (\phi_i)_{k-1} + \sum_{j \neq i}^{n} d_{ij} (\phi_j)_{k-1} \qquad (4.30)$$

Of course, this is the unnormalised form and all of the mixing coefficients will still need to be scaled to construct normalised molecular orbitals; however, the emphasis is that the self-contribution is constant and therefore the problems of finding n^2 optimum mixing coefficients reduces to finding $n(n-1)$ optimum mixing coefficients. Another reason for doing this (other than reducing number of variables) is that a linear dependence over the set used to form the new molecular orbital can form. Accordingly, the gradient and hessian elements of such self-contriubtions will be zero; but more importantly, one must remove these terms in order to prevent the construction of a singular hessian (a matrix with rows (and therefore columns) of zeros). Done carefully and correctly, the matrix of mixing coefficients is represented as a reshaped vector – of dimension $n(n-1)$ – with the elements of the one dimensional array ordered with the first row of the matrix mixing coefficients first

then the second row and so on (as opposed to column by column); this manoeuvre might seem pointless but the advantage is obvious when comparing the number of unique elements in the ordinary hessian — $\frac{n(n+1)}{2}$ — versus the contracted hessian — $\frac{p(p+1)}{2} : p = n(n-1)$. In the case of water, for example, which has five molecular orbitals, the number of unique hessian elements is reduced from 325 to 210. Finally, the measure of 'delocalisation percentage' is defined as [25]:

$$d_l = \left[\frac{1}{2} \int (\phi_l - \tilde{\phi}_l)^2 d\tau\right]^2 \tag{4.31}$$

$\tilde{\phi}_l$ is the localised molecular orbital constructed by erasing any non-local additions to the molecular orbital and renormalising.

It is no secret that there already exists research into the non-orthogonal localised molecular orbitals. Perhaps, the best of the previous results in this field was done by Yang *et al.* in a series of papers. Essentially, his approach is to maximise the Boys function by minimising the spread functional, Ω (with m equal to the number of electrons) [23][28][10]:

$$\phi_k = \sum_{i=1}^{m/2} \psi_i A_{ik} \tag{4.32}$$

$$\Omega[A] = \sum_{k=1}^{m/2} [\langle\phi_k|r^2|\phi_k\rangle - \langle\phi_k|r|\phi_k\rangle^2] \tag{4.33}$$

Which has an equal representation using the mixing coefficients (the NO-LMOs are functions of the coefficients after all):

$$\Omega[A] = \sum_{k=1}^{m/2} \{(A^\dagger R^2 A)_{kk} - (A^\dagger RA)_{kk} * (A^\dagger RA)_{kk}\} \tag{4.34}$$

$$R_{ij}^2 = \langle\psi_i|r^2|\psi_j\rangle$$

The spread functional is quite clearly the same as the Boys function whenever the set of orbitals in consideration is an orthonormal set; however, in his own words, "they will yield different results when the orthogonality condition is released." He continues to argue that the method is valid because a constraint on his NO-LMOs is that the centroids are forced to coincide with the centroids of the OLMOs which makes the set of final orbitals linearly independent. However, it is simply not fair to make these artificial conditions; our method, on the other hand, only requires that the wave-functions be made normalised after every update, which is a widely

accepted technique of quantum mechanics. In addition to this trick and optimising the spread functional rather than the Boys functional, the spread functional is transformed into yet another function:

$$\Omega[A] = \sum_{k=1}^{m/2} \{(A^\dagger R^2 A)_{kk} - (A^\dagger RA)_{kk}^2\}$$

$$= \sum_{k=1}^{m/2} \{a_k^\dagger R^2 a_k - (a_k^\dagger Ra_k)^2\} = \sum_{k=1}^{m/2} \omega[a_k] \qquad (4.35)$$

Which is a perfectly valid representation, the reasons for this are because in his method he aims to optimise each row of A independently which appears to be a valid argument; however, we disagree with his liberal use of the multiplier-penalty function method.

$$W[a_k, \lambda] = \omega[a_k] + \text{penalty parts [23][28][10]} \qquad (4.36)$$

The extra parts have Lagrange multipliers and involve terms of the three principal dipole directions (X,Y,Z); additionally, analytical gradient and hessian terms are calculated from this penalty function. The modified Newton method due to Gill and Murray was used to optimise the Lagrange multipliers of the penalty parts, and convergence of this iterative scheme was established once the following two conditions were met:

$$a_k^\dagger a_k = 1$$
$$\langle \phi_k | r | \phi_k \rangle - \langle \phi_k^0 | r | \phi_k^0 \rangle = 0 \qquad (4.37)$$

The first condition is the re-normalisation of the wave-functions, the latter is that the centroids of a given NO-LMO, ϕ_k, coincide with the corresponding one from an O-LMO, ϕ_k^0. The results are in some respect promising because the spread functional of their NO-LMOs are lower in value that the corresponding O-LMOs; additionally, they report positive definite hessians on convergence to a minimiser. However, a major flaw in their method is failure to report the final contribution of 'penalty parts'; one does not actually know if the error in this method is converging to error and if the modified functional is approaching the intended one. In summary, the author of this thesis believes the method of this thesis is better because it is much simpler to describe, the derivative information for the Boys function is exact, no contribution of error is made due to penalty functions, and no assumption about fixing the centroids is imposed.

4.1 Optimisation Methods

Often is the case in all flavours of applied mathematics – such as economics, physics, and chemistry – that many problems simply cannot be solved with a closed form answer. In the first chapter this idea was praised and humorously the opening quote scoffed at the idea of applying mathematics to chemistry; the fact is, the Schrdinger equation is a key equation of quantum chemistry like many others which cannot be solved that are equally 'simple' in their expression but nontrivial in their solutions. The Taylor series for an analytic function is around a change slight change in coordinates is:

$$f(x_n + \delta x) = f(x_n) + f'(x_n)\delta x + \frac{1}{2}f''(x_n)\delta x^2 + \cdots \tag{4.38}$$

The equation (4.38) should obtain a minimising/maximising solution, x^*, when its derivative is exactly zero. This motivates the use of the Newton-Raphson method which truncates (4.38) for terms higher than the second derivative, then differentiates the equation with respect to δx and attempts to find a root to the equation, $f'(x_n) + f''(x_n)\delta x = 0$ Guesses taken successively follow the general form, known as a line search Newton-like method [12, Chapter 3.1]:

$$x_{k+1} = x_k - \gamma H_k^{-1} g_k \quad : g_{k_i} = \frac{\partial f_k}{\partial i} \quad | \quad H = [h_k]_{i,j} \equiv \frac{\partial^2 f_k}{\partial i \partial j} \tag{4.39}$$

The non-negative scalar γ is chosen so as to further optimise the multidimensional problem in one dimension:

$$\phi(\gamma) \underset{\text{min/max}}{=} f(\gamma p_k + x_k) \quad p_k := \text{direction} \tag{4.40}$$

Explicit to its formulation, the hessian, H, is assumed to be non-singular and the gradient, g, should converge to zero as $x_k \to x^\star$. From now on we will speak of minimisation techniques; if one wishes to maximise a problem P, it is equivalent to minimising $-P$. One consequence of this (4.40) simple numerical method is that corrections to an approximation cannot occur if near or at a saddle point, where the gradient is zero but a local minima does not exist. In order for a value to be an optimal point it is necessary for the second order derivatives to be positive in every dimension, equivalently every eigenvalue must be positive. It can be easily shown that this would require every eigenvalue of the hessian to be positive because the non-singular hessian is similar $(A \sim B \Leftrightarrow \exists C : A = C^{-1}BC)$ to a diagonal matrix where each entry along its diagonal corresponds to a specific dimension of pairs of variables:

$$H = Q^{-1}\Lambda Q \tag{4.41}$$

$$H = \begin{pmatrix} \vec{q_i} & \cdots & \vec{q_m} \end{pmatrix} \begin{pmatrix} \lambda_1 & & 0 \\ & \ddots & \\ 0 & & \lambda_m \end{pmatrix} \begin{pmatrix} \vec{q_i} \\ \vdots \\ \vec{q_m} \end{pmatrix} \tag{4.42}$$

In particular, matrices which are similar have the same eigenvalues, moreover the entries of a diagonal matrix are its eigenvalues; therefore, the eigenvalues of H are the diagonal entries of Λ. We will not prove any of these results but a good text on useful results from finite dimensional linear algebra is provided by Axler [4]; these results are merely quoted without proof because they were especially useful and assumed in this research. Moreover, the decomposition we are interested in is known as eigenvalue-eigenvector decomposition (or spectral decomposition); wherein, Q is a matrix of row eigenvectors of H and $Q^{-1} = Q^T$ (due to the fact that eigenvector basis was chosen such that $q_i^T q_j = \delta_{i,j}$).

There is a serious issue in that, when the guess is really far from a local minimum it is almost surely going to converge to a saddle point. There are many different ways to fix this issue, but if the initial iterate is good – in some sense – then the following technique should work in theory [12, Chapter 3.1]:

$$\mathbb{H} = H + |\min\{\min(\sigma_H), 0\}| * I \tag{4.43}$$

$$p_k = -\gamma \mathbb{H}^{-1} g \quad : \gamma \geq 0 \tag{4.44}$$

σ_H denotes the eigenspectrum of the hessian. Observe that when the hessian is not sufficiently positive definite one then shifts the eigenspectrum by a sufficient amount to make the new modified matrix, $\mathbb{H}$, sufficiently positive definite; this doesn't change the set of eigenvectors so an eigenvalue eigenvector decomposition only needs to be performed once. As a result p_k becomes a direction of negative curvature because [30]:

$$p_k^T g \leq 0 \text{ and } p_k^T H_k p \leq 0 \tag{4.45}$$

These conditions on p will naturally be imposed if the hessian is positive definite and while there are many clever methods that exist to satisfy (4.45) other than (4.43) and (4.44), we believe the modification (4.43) to work particularly well. One obvious advantage of this method over others it that it is computationally very simple to define (4.43), while (4.44) would be a step carried out regardless. After finding this direction, one must still compute the step length, γ, which satisfies the one dimensional optimisation subproblem $\phi(\gamma)$. Finding the optimal solution is not surprisingly extremely difficult – even in this one dimension – because this would require a complete description of the one dimensional line. Therefore, we generally accept a coordinate, γ, which results in a decrease in the function [12, Chapter 2.5]:

$$f(x_{k+1}) := f(x_k + \gamma p_k) \text{ if } f(x_k + \gamma p_k) \leq f(x_k) \tag{4.46}$$

The case of equality is not a problem (ideally) because continuous evaluations should correct the function further. In practice, however, one wants a fast convergence, one which will reduce the function to a substantial degree; we would like to reduce the number of hessian evaluations but without completely minimising $\phi(\gamma)$. A good balance are the Wolfe conditions [12, Chapter 2.5]:

$$f(x_k + \gamma p_k) \leq f(x_k) + c_1 \gamma p_k^T g \tag{4.47}$$
$$p_k^T g(x_k + \gamma p_k) \geq c_2 p_k^T g \tag{4.48}$$
$$0 < c_1 < c_2 < 1$$

The first is known as the Armijo rule which aims to significantly reduce the function, while the second inequality is the curvature condition and encourages the slope of the function to deduce. The second condition is extremely important because it prohibits pathological searches that oscillate between sets of values which only slightly reduce the function; this can be seen, for example, in gradient like methods near a solution which zig-zag along 'valley structures'. Any starting point will converge under a gradient driven optimisation, but numerically (in finite time) the solution may never be found; the curvature condition helps ensure that such 'gradient-like' directions are not acceptable during the course of a line search. It has also been shown that the curvature condition is a bit weak, it can be made more robust through the following modification (known as the Strong Wolfe condition of curvature)[42][43]:

$$|p_k^T g(x_k + \gamma p_k)| \leq c_2 |p_k^T g| \tag{4.49}$$

The method commonly used to enforce these conditions is known as the backtracking line search. One first picks γ_0 and $\tau \in (0, 1)$ then updates $\gamma_l := \gamma_{l-1}\tau$ then updates until both of the inequalities are satisfied for a given γ_l. This is known as an inexact line search because $\phi(\gamma)$ is not actually minimised totally; moreover, if γ_0 is not chosen to be large enough then $\gamma_l \to 0$ and the line search fails completely. Obviously, one way around this problem is to then evaluate $\phi(\gamma)$ over a larger domain. In general, a good bracketing strategy is needed to pre-condition the subproblem for a sufficient line search; here the techniques of Fletcher were used [12, Chapter 2.6].

Another way to speed up computations without losing a significant amount of accuracy is to factor matrices that need to be inverted because, in general, matrix inversion is a costly procedure especially on a dense matrix of several dimensions. The Cholesky decomposition is a special type of LU-decomposition with $U = L^T$; additionally the Cholesky decomposition is always unique while the general LU-decomposition is never unique. The only rule for using the Cholesky decomposition is that the matrix being operated on must be positive definite. Some authors refer

to L as the matrix square root, however this is misleading because $L \neq L^T$; albeit, the algorithm does use square roots in its simplest form [18, Chapter 4.2]:

$$L_{j,i} = \sqrt{A_{j,j} - \sum_{k=1}^{j-1} L_{j,k}^2} \tag{4.50}$$

$$L_{i,j} = \frac{1}{L_{j,j}} \left(A_{i,j} - \sum_{k=1}^{j-1} L_{i,k} L_{j,k} \right) \quad : i > j \tag{4.51}$$

$$A = LL^T \tag{4.52}$$

Additionally, there is also a square root free (i.e. (4.50) free) method where $A = LDL^T$. While the square root can be seen as an opportunity to introduce error, it was often found that when taking the difference between our hessians and their decomposed versions, the error was on the order of machine epsilon. When it came to computing the inverse of the modified hessian times its gradient, $\mathbb{H}^{-1}g$, one can easily complete this with $(L^T)^{-1}(L^{-1})g$ because computing the inverse of a lower triangular matrix is simple and accurate. There were a number of other methods which were also investigated to see if they could potentially speed up the process of solving Boys equation more effectively than the method of (4.43). A large part of this research was devoted to testing these various methods to see what would work in practice and what the most efficient method available was. There exists a large portion of studies which suggests that Newton's method does not make full utility of second derivative information because it only generates a single direction. The 'Newton-like direction' or 'descent direction' is computed from a positive definite matrix, P:

$$s_k = -P_k^{-1} g_k \tag{4.53}$$

Without making any assumptions about P, we see that the Newton direction is very similar in form to the descent direction; in particular, if the hessian is positive definite, then one should use the hessian as the matrix for computing the descent direction. A direction of negative curvature is one such that:

$$d_k^T H d_k < 0 \tag{4.54}$$

Notice that d_k will always exist so long as there is at least one negative eigenvalue, to see this consider a unitary transformation on the hessian which diagonalises the eigenspectrum. Some of the methods perform a curve linear search for [30]:

$$x_{k+1} = x_k + \alpha^2 s_k + \alpha d_k \quad : \alpha > 0 \tag{4.55}$$

However, it has been suggested by others that this is prone to error as well as slow; there is a general philosophy in optimisation theory that one can try to 'over-optimise' a single step at the expense of time, when a less optimised method would

do the job cleaner and less expensively. In other words, more fast iterations may be better than a few slow 'better' iterations. The alternate choice is to construct the next iterate as [13][14]:

$$x_{k+1} = x_k + \alpha(s_k + \beta d_k) \quad : \alpha > 0 \tag{4.56}$$

$$\beta = \begin{cases} \left\{ -\frac{s^T H d}{d^T H d} + \sqrt{\left(\frac{s^T H d}{d^T H d}\right)^2 + 1 - \frac{s^T H s}{d^T H d}} \right\} & : d_k \neq 0 \text{ and } s^T H s \geq d^T H d \\ 0 & : \text{otherwise} \end{cases} \tag{4.57}$$

The exact methods used to compute s and d are different between various authors. Gill and Murray have suggested that the negative curvature be computed by a modified Cholesky decomposition; essentially, very similar to (4.43), a non-positive matrix is modified by shifting diagonal matrix such that is 'small' enough to make the new matrix positive definite:

$$H + E = LDL^T \tag{4.58}$$

$$R = L\sqrt{D} \tag{4.59}$$

$$\sigma(R) = \sigma(H + E) \quad \forall \lambda \in \sigma, \lambda > 0 \tag{4.60}$$

It is pragmatic to compute the direction of negative curvature using the shifted matrix technique (4.43), in practice it is found that other methods such as those suggested by Gill and Murray are too expensive at each iteration and the benefits are not worth the cost. All of these methods are definitely worth investigating; however, it was found that in the case of finding non-orthogonal localised molecular orbitals none of them worked. It could be that the 'initial guess' provided by ordinary Boy's calculations was not sufficient, as most eigenvalues of the coordinate hessian were positive but a few were negative – 2 to 3. The technique dual to the 'Line Search' treatment of the Taylor expansion is known as the 'Trust region' algorithm. The line search approach is to find a good direction (or directions) and minimise the objective function along the given line (or curve, in the case of linear combinations of directions); on the other hand, the trust region procedure is to find a good distance to travel from the current coordinate then find a direction given the 'good distance' and transfer the coordinates under some conditions. The 'line search' method is desirable for many reasons – its deep-rooted, its intuitive, and cheap – however it fails occasionally if the 'best' distance given a direction is far and the truncated Taylor expansion is no longer valid. The line search is good only if the distance is bounded, in some sense; this is the idea behind a trust region. Briefly, there is a small niche of optimisation theory which considers higher order Taylor expansions; it is possible that the third derivative tensor methods like Halley's method are better suited for line searches however this is both computationally and algorithmically complex.

4.2 Trust Region Methods

The trust region (or restricted step) problem can be summarised as follows, find [12, Chapter 5]

$$p_k \quad ||p_k||_2 \leq \Delta \tag{4.61}$$

Where Δ^2 is the trust region, an open ball of n-dimensions centred at the current position, x_0, contains the set of vectors which satisfy this criteria:

$$\mathcal{B} = \{x : ||x_0 - x|| \leq \Delta\} \tag{4.62}$$

However, this is not a simple problem because unlike the case of the line search where an n-dimensional problem is reduced to a 1-D problem, a trust 'ball' is still n-dimensional and there is no obvious choice for the 'best direction'. One can rewrite the second order truncated Taylor expansion as a quadratic equation [12, Chapter 5]:

$$f(x_0 + \delta) \approx Q(\delta) := f(x_0) + \delta^T g + \frac{1}{2}\delta^T H \delta \tag{4.63}$$

The trust region problem then becomes rephrased as:

$$\min Q(\delta) \text{ subject to } ||\delta||_2 \leq \delta, \delta \in \mathbb{R}^n \tag{4.64}$$

$$\text{moreover as } \delta \to \delta^\star, \quad Q(\delta) \leq 0 \tag{4.65}$$

It can be shown that any minimiser of the above equation restricted to the boundary of the ball will satisfy [12, Chapter 5]:

$$H + \nu^\star I \equiv H(\nu^\star) \quad : H(\nu^\star)s^\star = -g \tag{4.66}$$

$$\infty > \nu^\star \geq 0$$

$$\nu \cdot (||s^\star|| - \Delta) = 0 \tag{4.67}$$

$$\psi(\nu) = s^T s - \Delta^2 = 0 \tag{4.68}$$

Where $H(\nu^\star)$ is positive semidefinite, if $H(\nu^\star)$ is positive definite then $s^\star$ is unique. The question then becomes one of finding $\nu^\star$ in order to find $s^\star$ given the restrictions imposed by Δ. Further, it is clear that this is a highly non-linear problem. There are many ways of finding the correct shift, but essentially this becomes another nested optimisation problem; first one must properly bracket off where $\nu^\star$ should be, before finding it. After upper and lower bounds are set for finding $\nu^\star$, one should seek solutions of $\nu^\star$ using means which are simple, such as the bisection method or the golden section search. It is the opinion of the author that that a one-dimensional

Newton method is more efficient and in fact simple to calculate. Suppose that our hessian has a spectral decomposition $H = Q^T \Lambda Q$ then it follows that:

$$H(\nu) = Q^T(\Lambda + \nu I)Q \tag{4.69}$$

$$\nu^\star > \min(0, -\min(\sigma(H))) \tag{4.70}$$

$$s(\nu) = -H(\nu)^{-1}g = -Q^T(\Lambda + \nu I)^{-1}Qg \tag{4.71}$$

Equation (4.70) can be proven but we will not show it here, while equation (4.71) has the brilliant property that the inverse of a spectral decomposition is analytical – one simply needs to find the scalar inverse of every element of the diagonal matrix $(\Lambda + \nu I)$. Rather than directly dealing with the case of finding $s(\nu)$ such that $||s(\nu)||_2^2 = \Delta$ – which is a tough non-linear, non-convex problem – one can transform the problem into a simple problem with a clean first derivative and strictly increasing after the solution [37]:

$$\phi(\nu) := \frac{1}{||s(\nu)||_2^2} - \frac{1}{\Delta} \tag{4.72}$$

$$\phi'(\nu) = \frac{s(\nu)H^{-1}s(\nu)}{||s(\nu)||_3^2} \tag{4.73}$$

$$\nu_{k+1} = \nu_k - \phi(\nu)\phi'^{-1}(\nu) \tag{4.74}$$

The function is particularly pleasant because for $\nu > \min(\sigma(H))$, $\phi(\nu)$ is monotonically increasing and concave. The norm of $s_(\nu)$ is also easily computed given that the rotation matrix Q is an isometry:

$$||s(\nu)||_2 = ||Q^T(\Lambda + \nu I)^{-1}Qg||_2 = ||Q^T(\Lambda + \nu I)^{-1}Qg||_2 = \sqrt{\sum_{i=1}^{n} \frac{[Qg]_i}{\lambda_i + \nu}} \tag{4.75}$$

Clearly all the components can be calculated very rapidly so that $s^T s \to \Delta^2$ as $\nu_k \to \nu^\star$ and our solution to the trust region problem is very clear. Because of the definite hessian we can decompose accelerate computation through the Cholesky factorisation. Moreover, we have the following [6, Chapter 4]:

$$\langle s(\nu)|H^{-1}s(\nu)\rangle = \langle L^{-1}s|L^{-1}s\rangle = ||\omega||^2 \quad : \omega \equiv L^{-1}s \tag{4.76}$$

$$s = -L^{-1}L^{-T}g \tag{4.77}$$

$$\omega = L^{-1}s \tag{4.78}$$

$$\nu_{k+1} = \nu_k + \left(\frac{||s(\nu)||_2 - \Delta}{\Delta}\right)\left(\frac{||s(\nu)||_2^2}{||\omega||_2^2}\right) \tag{4.79}$$

It is not necessary for one to do the Cholesky decomposition after computing the eigenvalues and shifting, as this is only one option; alternatively, $\phi'(\nu)$ can be computed as:

$$\phi'(\nu) = \frac{s(\nu)H^{-1}s(\nu)}{||s(\nu)||_2^3} = \frac{(Qg)^T(\Lambda + \nu I)^{-3}(Qg)}{||s(\nu)||_2^3} \tag{4.80}$$

This is straight forward to show true, given the definition of $H(\nu)$ and the fact that a decomposition exists. This approach has the advantage over using the Cholesky decomposition because one is shifting the Hessian – after computing eigenvalues and eigenvectors – followed by the extra decomposition, finding explicitly s and its norm, as well as ω. The disadvantage is the extra assurance one receives through a successful Cholesky decomposition which is only ensured on positive definite hessians.

There is only one caveat, we have yet to define the bounds on this method and any convergent method should start in a good domain. Because of the Geršgorin circle theorem, we can put exact (analytical) limits on the domain of [6, Chapter 4]:

$$\nu_0 = \max[\sqrt{\nu_L \nu_U}; V_L + .01(\nu_U - \nu_L)] \tag{4.81}$$

A fair and natural query is 'why bother with this complex Newton method when something simple like the bisection method will work?'; fortunately, there is realistic trade off. To the best of the author's knowledge there is no published suggestion to use the secant method to solve $\phi(\nu)$ The secant method is a finite differences approximation to the Newton-Raphson method. It has a convergence rate equal to the golden ratio – not quite as fast as Newton's method – but is faster than Newton's method per iteration because it does not involve extra computations as discussed above. The Secant method:

$$\nu_k = \nu_{k-1} - \phi(\nu_{k-1})\frac{\nu_{k-1} - \nu_{k-2}}{\phi(\nu_{k-1}) - \phi(\nu_{k-2})} \tag{4.82}$$

on average converges in about 7 to 8 iterations, in contrast to the bisection method which typically took at least 20 iterations. In some sense, the secant and Newton methods are risky because they have no bracketed domain which is updated – as in the case of the bisection method – therefore there is always the possibility that a value for $\nu < 0$ can be found. A puerile yet effective way around this is to always choose the first pair of values for the secant method (ν_0, ν_1) to be very large so that convergence is guaranteed. An illustration of the plots of $\psi(\nu)$ and $\phi(\nu)$ is given to compare the chaotic nature of the first function with the calmed behaviour of the latter.

Figure 4.1: Plots of the Trust Region sub-problem function
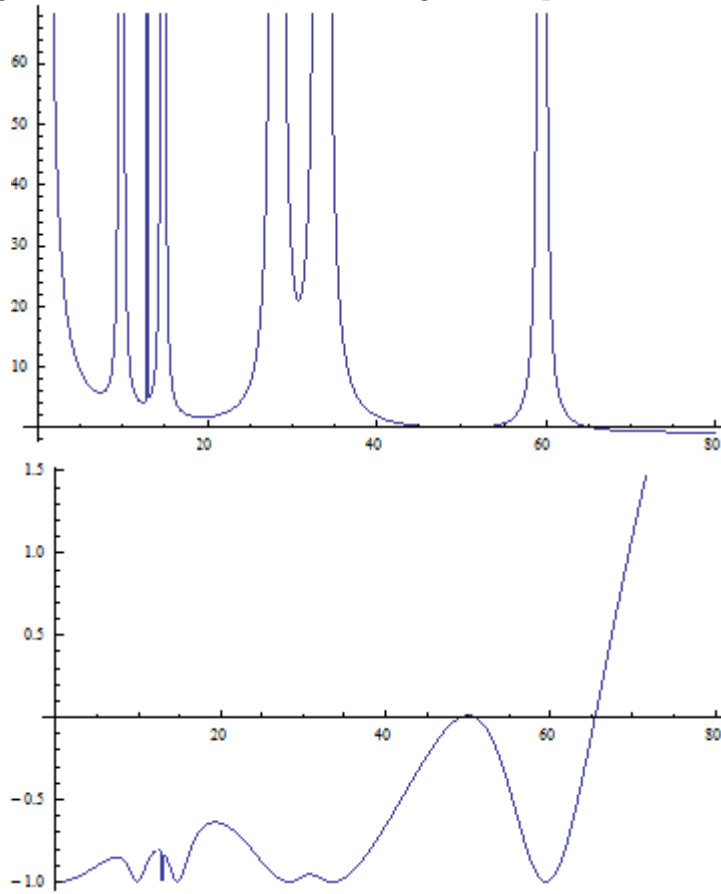
These plots were made using the initial hessian and gradient of the Boys NOLMO problem for water over various values of ν, setting Δ to 1, within the Mathematica 8.0 environment. The three roots of each function coincide, however it is clear that the second function is easier to optimise because it is monotonically increasing after the third root; additionally, one can clearly see that the bisection method may fail under certain conditions. Namely, if the initial pair of values (ν_0, ν_1) do not have opposite signs for their given function, then the bisection method will never converge. Looking at the graphs, it is clear that even if one value is chosen arbitrarily large that the other value needs to be chosen so its function's sign is negative, which may be difficult to do because of unexpected extra roots and the extra domain of positive values. Namely, there appear to be two unexpected roots between 40 and 60, for a different value of Δ these roots would disappear or become exaggerated; we would like to find root invariant to subtle changes in Δ, which is resolved by using the secant method approaching from the far right. Also notice that an increase in the value

of the trust region would result in 'nearly similar solutions for ν' being pushed left, corresponding to slightly lower values of ν. In the limiting situation, as Δ becomes larger there may appear more roots; this should be expected as this corresponds to more minimising directions accepted, those with the given magnitude. However, the bisection method could pick a bad initial pair (in which case, a new pair must be selected) or it could pick a root like that between 40 and 60.

Both the 1-D Newton and secant iteration are inexpensive because the inverse of the shifted hessian must be calculated regardless for the purpose of checking convergence, this information might as well be employed to accelerate convergence rather than just testing it. So far we have talked about the so called 'trust region' in a very intangible way, essentially the trust region is updated in a way that the algorithm remains restricted yet robust. The ratio between the actual reduction in a function and its predicted quadratic reduction is measured as [12, Chapter 5]:

$$\rho = \frac{f(x_0) - f(x_0 + \delta)}{Q(0) - Q(\delta)} \tag{4.83}$$

$$\text{if } \rho \leq \kappa_\alpha : \quad x_{k+1} = x_k \text{ and } \Delta_{k+1} := \frac{\Delta_k}{2}$$

$$\text{if } \kappa_\alpha < \rho < \kappa_\beta : \quad x_{k+1} = x_k + s \text{ and } \Delta_{k+1} := \Delta_k$$

$$\text{if } \rho \geq \kappa_\beta : \quad x_{k+1} = x_k + s \text{ and } \Delta_{k+1} := 2\Delta_k$$

The choice for κ_α and κ_β ($0 < \rho < 1$) is particular to the problem at hand; in actuality, one may even choose a more sophisticated set of rules, involving more than three criteria. Essentially the idea is that if the quadratic approximation to the trust region is poor then we should reevaluate what we consider 'safe' and restrict ourselves to a smaller region of the Taylor expansion; then again, if the ratio is approaching unity then we can assume the higher order terms provide little correction and we make our trust region less conservative.

Finally, it is appropriate to discuss the Broyden–Fletcher–Goldfarb–Shanno (BFGS) method, because a slightly modified version of it is used as default for standard geometry calculations in the Gaussian environment [12, Chapter 3.2]. If one were think of the domain of our variables as having regions with positive definite hessians and those without positive definite hessians, then it is correct to consider our problem of minimising our function in two parts. In the first half of optimisation, our modification to the hessian is an attempt to approach a coordinate domain associated with a hessian which is positive definite in its own right. In the second half of optimisation, we simply want to find the minimising coordinates within this subdomain. At this point, one can imagine cutting this domain out of the full space and considering only how to find its minimum. Here, a method should be used which is fast, reliable, and does not leave domain; the BFGS method is perfectly suited to solve a sufficiently

good approximation.

BFGS Algorithm

    i $\mathfrak{H}_0 = H$, provided $\min(\sigma_H) > +10^{-6} \Leftrightarrow H$ is sufficiently positive definite

    ii $\mathfrak{H}_0^{-1} = (L^T)^{-1}(L^{-1}I)$: $H = LL^T$; set $k = 0$

    iii $p_k = -\mathfrak{H}_k^{-1} g_k$

    iv $x_{k+1} = x_k + \gamma p_k \Leftarrow f(x_{k+1}(\gamma)) = \min_\gamma (x_k + \gamma p_k)$

    v $y_k = g(x_{k+1}) - g(x_k)$

    vi $\mathfrak{H}_{k+1} \overset{\text{def}}{=} \mathfrak{H}_k + \frac{y_k \otimes y_k}{y_k^T s_k} - \frac{\mathfrak{H}_k * (s_k \otimes s_k) * \mathfrak{H}_k}{s_k^T \mathfrak{H}_k s_k}$

    vii $\mathfrak{H}_{k+1}^{-1} \overset{\text{def}}{=} \mathfrak{H}_k^{-1} + \frac{(y_k^T s_k + y_k^T \mathfrak{H}_k^{-1} y_k)(s_k \otimes s_k)}{(y_k^T s_k)^2} - \frac{\mathfrak{H}_k^{-1}(y_k \otimes s_k) + (s_k \otimes y_k)\mathfrak{H}_k^{-1}}{y_k^T s_k}$

    viii Return to iii and repeat until $g \leq \epsilon$, $|f(x_{k+1}) - f(x_k)| \leq \epsilon$, and $||x_{k+1} - x_k|| \leq \delta$

    ix Confirm that the final analytical hessian is sufficienty positive definite

Here the author used $\otimes$ to emphasise the outer product. In the first step, $\mathfrak{H}_0$ is set to equal the exact positive definite Hessian; obviously, there is no guarantee that the hessian should be positive definite in general. However, given a positive definite hessian this method will maintain that property; otherwise, setting $\mathfrak{H}_0$ to identity or some weighted diagonal will work, which is common in the case of geometry calculations.

4.3   Future Research

The dynamic evolution of overlap integrals through a reaction pathway (such as the IRC) is an especially interesting approach to analysing the progression of a chemical reaction because chemical reactions can be thought of as nothing more than reorientation of groups of electrons with respect to one another and their associated molecular orbitals. Even though the research contained in this thesis does not include any quantum chemical computation of this type, it would be interesting to merge the algorithms of Boys' non-orthogonal totally localised molecular orbitals with the intrinsic reaction coordinate calculation. This would simply mean that for every given number of steps along the reaction pathway a full Boys calculation would be performed; alternatively one could require, for example, a significant change in

energy to occur before performing another Boys procedure. If the computation is updated regularly enough, the initial set of mixing coefficients for a given step could be the final set of mixing coefficients for the previous step.

A large part of this thesis was exclusively devoted to the stating the Boys localisation problem and analysing various potential numerical methods to find one which worked; remarkably, there exists another function very similar to Boys functional which has received very little attention in texts, online communities, or academic journals. The so called exclusive molecular orbitals also maximise the centroids of electronic charge, equivalent to maximising the following functional:

$$\langle \Omega \rangle' = \frac{1}{2} \prod_{i \neq j}^{n} \left(\frac{\langle \psi_i' | r | \psi_i' \rangle}{\langle \psi_i' | \psi_i' \rangle} - \frac{\langle \psi_j' | r | \psi_j' \rangle}{\langle \psi_j' | \psi_j' \rangle} \right)^2 \tag{4.84}$$

Chapter 5

Conclusions

The research contained within this thesis was primarily devoted to describing the Diels-Alder reaction of 2,4–hexadiene with sulfur dioxide while presenting the general theory that underlies the means for performing such calculations. This reaction was shown to have a very concerted mechanism as per the IRC calculations and highly suggestive TS localised molecular orbitals; for this reason, the author insists that if a mechanism is to be proposed, it should depict homolytic bond cleavage. Energies reported are in good agreement with the literature [41]. The geometries for each structure along the reaction path are optimised and compared using MP2 and B3LYP methods. Additionally, basis set superposition error was shown to contribute very little to this reaction's geometry; not surprisingly, BSSE was shown to have an appreciable contribution to the energy of the system.

Our investigation of optimising the Boys functional is to date partially sucessful so this puts it in good light. Using water as our model system, we were able to optimise the mixing coefficients such that the Hessian is sufficiently positive definite and the norm of the gradient is less than 1. Unfortunately, some of the off-diagonal elements of the overlap matrix are approaching +1, this is associated with different molecular orbital centroids coinciding, which is unacceptable. Recently, we suspect that performing a constrained optimisation – for a given fixed determinant value – may force the linear independence of the molecular orbitals. Over various values for any given determinant value one could select the best results so that the localised molecular orbitals are both optimised and natural. We have tested various unconstrained non-linear optimisation algorithms, which manipulate second-order information more efficiently than equation (4.43) combined with a simple line search. Currently we are concerned with finding a solution without nonsensical results; however, practically, it would be desirable to pick the most efficient method after we obtain sound results.

Our method is distinct from that of Yang *et al.* [23][28][10] in that we do not assume that the centroids of the localised molecular orbitals should be fixed nor do we transform the Boys functional to equation (4.35) followed by the addition of penalty functions. While Yangs's method does produce somewhat pleasant results, it is not accurate to consider such results as optimised. In the same manner, the ordinary Boys solution is not mathematically optimised and is therefore unsatisfactory for the same reasons. Just as Yang's and our method uses the non-optimal solution from Boys method, an alternative approach may be to apply our methods to Yang's 'solution'. This technique may precisely avoid the linear dependence of our molecular orbitals and give satisfactory overlap matrix elements. While inchoate, this and the constrained determinant method may be tested, with the best method used in the future.

Bibliography

[1] G09 keyword: Irc. `http://www.gaussian.com/g_tech/g_ur/k_irc.htm`, September 2011.

[2] G09 keyword: Opt. `http://www.gaussian.com/g_tech/g_ur/k_opt.htm`, November 2011.

[3] G09 keyword: Scf. `http://www.gaussian.com/g_tech/g_ur/k_scf.htm`, September 2011.

[4] S. J. Axler. *Linear Algebra Done Right*. Springer-Verlag New York, second edition, 1999.

[5] R. J. Bartlett and D. M. Silver. Manybody perturbation theory applied to electron pair correlation energies. I. closedshell firstrow diatomic hydrides. *J. Chem. Phys.*, 62(3258), 1975.

[6] F. V. Berghen. *CONDOR: a constrained, non-linear, derivative-free parallel optimizer for continuous, high computing load, noisy objective functions.* PhD thesis, Université Libre de Bruxelles, 2003-2004.

[7] Z. Z. bo and S. Z. an. An efficient technique for obtaining eigenvectors of a hamiltonian in a basis of non-orthogonal orbitals. *J. Phys. A*, 21(12), March 1988.

[8] B. Bradie. *A Friendly Introduction to Numerical Analysis*. Pearson Education International, 2006.

[9] S. H. Cheng and N. J. Highman. A modified cholesky algorithm based on a symmetric indefinite factorization. *SIAM J. Matrix Anal. Appl.*, 19(4):1097–1110, October 1998.

[10] G. Cui, W. Fang, and W. Yang. Efficient construction of nonorthogonal localized molecular orbitals in large systems. *J. Phys. Chem. A*, 114:8878–8883, June 2010. Part of the 'Klaus Ruedenberg Festschrift'.

[11] O. Diels and K. Alder. Synthesen in der hydroaromatischen reihe. *Justus Liebigs Annalen der Chemie*, 460:98–122, 1928.

[12] R. Fletcher. *Practical Methods of Optimization*. Wiley-Interscience, second edition, 1987.

[13] A. Forsgren, P. Gill, and W. Murray. Computing modified newton directions using a partial cholesky factorization. *SIAM J. Sci. Comput.*, 16(1):139–150, 1995.

[14] A. L. Forsgren, P. E. Gill, and W. Murray. A modified newton method for unconstrained minimization. Systems optimization laboratory (SOL), Standford University: Department of Operations Research, Stanford, CA 94305, September 1989.

[15] J. M. Foster and S. F. Boys. Canonical configurational interaction procedure. *APS:Reviews of Modern Physics*, 32(2):300–302, April 1960.

[16] K. Fukui. The path of chemical reactions - the irc approach. *Accounts of Chemical Research*, 14(12):363–368, December 1981.

[17] T. L. Gilbert. *Molecular Orbitals in Chemistry, Physics, and Biology: A Tribute to R. S. Mulliken.* Self-Consistent Equations for Localized Orbitals in Polyatomic Systems. Academic Press, 1964.

[18] G. H. Golub and C. F. V. Loan. *Matrix Computations.* The John Hopkins University Press, second edition, 1989.

[19] N. I. Gould, M. R. Stefano Lucidi, and P. L. Toint. Exploiting negative curvature directions in linesearch methods for unconstrained optimization. Technical report, Department for Computation and Information; Atlas Centre; Rutherford Applleton Laboratory, Oxfordshire OX11 0QX, December 1997.

[20] J. G. Hill, D. L. Cooper, and P. B. Karadakov. Spin-coupled description of aromaticity in the retro diels-alder reaction of norbornene. *J. Phys. Chem. A*, 112:1282312828, 2008.

[21] H. P. Hratchian and H. B. Schlegel. Accurate reaction paths using a hessian based predictor-corrector integrator. *J. Chem. Phys.*, 120:9918–9924, 2004.

[22] H. P. Hratchian and H. B. Schlegel. Using hessian updating to increase the efficiency of a hessian based predictor-corrector reaction path following method. *J. Chem. Theory and Comput.*, 1:61–69, 2005.

[23] L. L. Huasheng Feng, Jiang Bian and W. Yang. An efficient method for constructing nonorthogonal localized molecular orbitals. *AIP: The Journal of Chemical Physics*, 120(9458):9458–9466, 2004.

[24] F. Jensen. *Introduction to Computational Chemistry*. John Wiley and Sons, 1999.

[25] D. A. Kleier, T. A. Halgren, J. H. Hall, and W. N. Lipscomb. Localized molecular orbitals for polyatomic molecules. i. a comparison of the edmiston-ruedenberg and boys localization methods. *J. Chem. Phys.*, 61(3905), 1974.

[26] J. Lennard-Jones. The electronic structure of some diatomic molecules. *Trans. Faraday Soc.*, 25:668–686, September 1929.

[27] I. N. Levine. *Quantum Chemistry*. Prentice Hall, fifth edition, 2000.

[28] S. Liu, J. M. Pérez-Jordá, and W. Yang. Nonorthogonal localized molecular orbitals in electronic structure theory. *Journal of Chemical Physics*, 112(4):1634–1644, January 2000.

[29] C. Møller and M. Plesset. Note on an approximation treatment for many-electron systems. *Physical Review*, 46:618–622, October 1934.

[30] J. J. Moré and D. C. Sorensen. On the use of directions of negative curvature in a modified newton method. *Mathematical Programming*, 16(1):1–20, 1979.

[31] C. Peng, P. Y. Ayala, H. B. Schlegel, and M. J. Frisch. Using redundant internal coordinates to optimize equilibrium geometries and transition states. *J. Comp. Chem.*, 17(49), 1996.

[32] J. Pipek and P. G. Mezey. A fast intrinsic localization procedure applicable for *ab initio* and semiempirical linear combination of atomic orbital wave functions. *J. Chem. Phys.*, 90(9), May 1989.

[33] J. A. Pople, J. S. Binkley, and R. Seeger. Theoretical models incorporating electron correlation.

[34] G. C. Schatz and M. A. Ratner. *An Introduction to quantum mechanics in chemistry*. Prentice Hall, 2001.

[35] H. B. Schlegel. Optimization of equilibrium geometries and transition structures. *J. Comp. Chem.*, 3:214–218, 1982.

[36] R. B. Schnabel and E. Eskow. Software for a new modified cholesky factorization. Technical report, University of Colorado at Boulder: Department of Computer Science, August 1989.

[37] D. C. Sorensen. Newton's method with a model trust region modification. *SIAM J. on Numerical Analysis*, 19(2):409–426, April 1982.

[38] P. J. Stephens, F. J. Devlin, C. F. Chabalowski, and M. J. Frisch. *Ab Initio* calculation of vibrational absorbtion and circular dichroism spectra using density functional force fields. *The Journal of Physical Chemistry*, 98(45):11623–11627, November 1994.

[39] A. Szabo and N. S. Ostlund. *Modern Quantum Chemistry: Introduction to Advanced Electronic Structure Theory*. Macmillan Publishing Co., 1982.

[40] W.-C. Tung, M. Pavanello, and L. Adamowicz. Accurate one-dimensional potential energy curve of the linear $(H_2)_2$ cluster. *J. Chem. Phys.*, 133(124106), 2010.

[41] W. Wen-Feng, Z. Yong-Fan, and L. Jun-Qian. Dft study on the mechanism of cheletropic addition of SO_2. *Acta Phys. Chim. Sin*, 22(1):82–85, January 2006. Article in Chinese Characters.

[42] P. Wolfe. Convergence conditions for ascent methods. *SIAM Rev.*, 11:226–235, 1969.

[43] P. Wolfe. Convergence conditions for ascent methods II: Some corrections. *SIAM Rev.*, pages 185–188, 1971.